ELSEVIER

Seminars in
NUCLEAR
MEDICINE

PET/CT Variants and Pitfalls in Head and Neck Cancers Including Thyroid Cancer

Jasna Mihailovic, MD, PhD,[*,†] Ronan P. Killeen, FFR(RCSI) ABNM,[‡,§] and John A. Duignan, FFR(RCSI)[‡,§]

PET/CT imaging is a dual-modality diagnostic technology that merges metabolic and structural imaging. There are several currently available radiotracers, but ^{18}F-FDG is the most commonly utilized due to its widespread availability. ^{18}F-FDG PET/CT is a cornerstone of head and neck squamous cell carcinoma imaging. ^{68}Ga-DOTA-TOC is another widely used radiotracer. It allows for whole-body imaging of cellular somatostatin receptors, commonly expressed by neuroendocrine tumors and is the standard of reference for the characterization and staging of neuroendocrine tumors.

The normal biodistribution of these PET radiotracers as well as the technical aspects of image acquisition and inadequate patient preparation affect the quality of PET/CT imaging. In addition, normal variants, artifacts and incidental findings may impede accurate image interpretation and can potentially lead to misdiagnosis. In order to correctly interpret PET/CT imaging, it is necessary to have a comprehensive knowledge of the normal anatomy of the head and neck and to be cognizant of potential imaging pitfalls. The interpreter must be familiar with benign conditions which may accumulate radiotracer potentially mimicking neoplastic processes and also be aware of malignancies which can demonstrate low radiotracer uptake.

Appropriate use of structural imaging with either CT, MR or ultrasound can serve a complimentary role in several head and neck pathologies including local tumor staging, detection of bone marrow involvement or perineural spread, and classification of thyroid nodules. It is important to be aware of the role of these complementary modalities to maximize diagnostic accuracy and patient outcomes.

The purpose of this article is to outline the basic principles of PET/CT imaging, with a focus on ^{18}F-FDG PET/CT and ^{68}Ga-DOTA PET/CT. Basic physiology, variant imaging appearances and potential pitfalls of image interpretation are presented within the context of common use cases of PET technology in patients with head and neck cancers and other pathologies, benign and malignant.

Semin Nucl Med 51:419-440 © 2021 Published by Elsevier Inc.

Introduction

Combined PET/CT imaging represents a fusion of both anatomical and metabolic data. It offers several advantages over PET imaging alone including a significant reduction in image acquisition time, anatomical correlation, and more accurate localization of focal areas of increased radiotracer uptake within detected lesions.

^{18}F is the most frequently used radiotracer for PET/CT imaging as it has a long half-life of 110-minute and is available to many nuclear medicine centers worldwide. ^{18}F-labelled 2-deoxy-2-D-glucose (Fluorodeoxyglucose or FDG) is the most applied PET tracer for oncology imaging, in which the hydroxyl group of glucose is replaced by a positron-emitting fluorine isotope.

^{68}Ga-DOTAPET/CT is an imaging technique for the detection and characterization of neuroendocrine tumors (NETs). ^{68}Ga can be used to image somatostatin receptor expression

*Department of Radiology, Faculty of Medicine, University of Novi Sad, Novi Sad, Serbia.
†Centre of Nuclear Medicine, Oncology Institute of Vojvodina, Sremska Kamenica, Serbia.
‡Department of Radiology, St Vincent's University Hospital, Elm Park, Dublin 4, Ireland.
§UCD — SVUH PET CT Research Centre, St Vincent's University Hospital, Elm Park, Dublin 4, Ireland.
Address reprint requests to Jasna Mihailovic, MD, PhD, Prof, Department of Radiology, Faculty of Medicine, University of Novi Sad, Hajduk Veljkova 3, 21000, Novi Sad, Serbia. E-mail: jasna.mihailovic@mf.uns.ac.rs

https://doi.org/10.1053/j.semnuclmed.2021.03.002
0001-2998/© 2021 Published by Elsevier Inc.

and is vastly superior to ^{111}In labeled octreotide studies.[1] ^{68}Ga is produced in an onsite generator as it has a short half-life of 68 minutes. It is then chelated to either octreotide (^{68}Ga-DOTA-TOC or ^{68}Ga-DOTA-NOC) or octreotate (^{68}Ga-DOTA-TATE) using the organic compound DOTA (1,4,7,10-tetraazacyclododecane-1,4,7,10-tetraacetic acid).[2] This is a much more complex process than preparation of ^{18}F-FDG and so this radiotracer is not as widely available.

Basic Physiology

Increased glucose uptake in tumor cells is a result of increased anaerobic glycolysis, known as the Warburg effect. Cancer cells express an increased number of specific glucose transporter proteins compared to normal tissue cells. Following administration, FDG, like glucose is taken up from the plasma by tumor cells via these facilitative glucose transporter proteins (GLUTs). FDG is then phosphorylated by the enzyme hexokinase and converted into FDG-6-phosphate. Expression of GLUTs and hexokinase, as well as the affinity of hexokinase for phosphorylation of glucose or FDG is generally higher in cancer cells than in normal cells. Glucose-6-phosphate travels farther down the glycolytic or oxidative metabolic pathway in contrast to FDG-6-phosphate, which cannot be metabolized. In normal cells, glucose-6-phosphate or FDG-6-phosphate can be dephosphorylated and exit the cells. In cancer cells, however, expression of glucose-6-phosphatase is usually significantly decreased, and glucose-6-phosphate or FDG-6-phosphate is only minimally dephosphorylated and remains within the cell. FDG-6-phosphate cannot be metabolized and therefore does not follow the glucose metabolism route any further – it is metabolically trapped inside of the tumor cells. This process of "metabolic trapping" of FDG within the cell constitutes the basis for ^{18}F-FDG PET/CT imaging. Diagnosis of malignant tumors is therefore a major indication for ^{18}F-FDG PET−CT imaging.[3-7]

Neuroendocrine cells control various physiological processes by secreting hormones. These hormones bind inhibitory or stimulatory cell surface receptors. The most ubiquitous inhibitory cell surface receptor is the somatostatin receptor (SSTR), of which there are 5 subtypes. The peptide somatostatin and various synthetic somatostatin analogues, including octreotide can be used to bind SSTR.[8]

This allows whole body imaging of cellular SSTR expression and is the standard of reference for the characterization of NETs. Little difference has been demonstrated in clinical utility between each analogue (^{68}Ga-DOTA-TOC, ^{68}Ga-DOTA-NOC or ^{68}Ga-DOTA-TATE) and the decision is most often driven by local availability.[9]

Common Uses of PET CT in Head and Neck Cancer Evaluation

^{18}F-FDG PET/CT is recommended for the initial staging of advanced head and neck squamous cell carcinoma (HNSCC) – stage III and IV disease, to detect distant metastases.[10] It can detect metastases in approximately 15% of patients with advanced disease and alter management in up to 31% of cases.[11] Despite the high accuracy of ^{18}F-FDG PET/CT for the detection of metastases in patients with HNSCC (sensitivity of 88% and specificity of 94%), it remains underutilized for this purpose.[12,13]

^{18}F-FDG PET/CT can also be used to identify the primary tumor site in patients with malignant cervical adenopathy of unknown primary. In this context ^{18}F-FDG PET/CT can detect a primary lesion in up to a third of cases.[14]

Other important uses of PET/CT include radiotherapy planning, post treatment evaluation and assessment of disease recurrence. The PET-NECK trial demonstrated non-inferior outcomes for patients who underwent ^{18}F-FDG PET/CT 12 weeks post chemo-radiotherapy compared to those that underwent neck dissection for N2/3 disease.[15] A negative 12-week ^{18}F-FDG PET/CT offers good prognostic reassurance, and has been incorporated in the National Comprehensive Cancer Network (NCCN) guidelines.[16]

Given the extensive use of ^{18}F-FDG PET/CT in head and neck cancer, it is of paramount importance that the reader of PET/CT is aware of the many variants, pitfalls and artifacts that may hamper interpretation.

Patient Preparation

Adequate patient preparation is necessary to optimize the utility of ^{18}F-FDG PET/CT or ^{68}Ga-DOTAPET/CT imaging. For ^{18}F-FDG PET/CT patients are advised to fast approximately 4-6 hours before image acquisition and to abstain from beverages with sugar. This ensures FDG uptake by tumor cells, which may be reduced if glucose levels are increased due to glucose-FDG competition. Additionally, the dominant myocardial metabolism of fatty acids in the fasting state reduces FDG uptake in myocardium. Fasting is not required prior to ^{68}Ga-DOTA PET/CT. It has been recommended by some authors to discontinue octreotide therapy to avoid SSTR blockade but many centers do not require this. An option to minimize their effect is to perform ^{68}Ga-DOTA PET/CT the day before administration of a long acting octreotide agent.[17]

Knowledge of the patient's medical history is necessary with particular attention to the following; a full treatment history including timing of chemotherapy, external radiation therapy, administration of bone marrow stimulating factors, recent octreotide therapy, recent surgery or biopsy, prior diagnostic imaging and relevant lab analysis.

Image Acquisition

The European Association of Nuclear Medicine (EANM) has published guidelines for optimal ^{18}F-FDG PET/CT and ^{68}Ga-DOTAPET/CT imaging.[17,18] The patient's blood glucose level is checked prior to ^{18}F-FDG PET/CT with recommended values of 120-150 mg/dL. The EANM recommend a dose

calculation based on the patient's weight and the degree of table overlap at each table position during image acquisition (greater or less than 30%). This ensures consistency in SUV-max values between different institutes or even within the same patient as their weight may change over the course of treatment. It allows for a standardized approach to diagnosis, staging and treatment response.[18]

If diabetic patients demonstrate glucose levels of greater than 200-250 mg/dL, they should be rescheduled, rather than intravenously treated by insulin which can increase FDG uptake in fat and muscles and compromise image interpretation. PET/CT imaging is performed about 60-90 minutes after intravenous ^{18}F-FDG radiotracer administration and after 45-90 minutes in the case of ^{68}Ga-DOTA.

Following application of the ^{18}F-FDG radiotracer, patients are placed in a quiet room with instructions to rest, stay calm without excessive movement to minimize skeletal muscle uptake. To avoid possible brown fat activation, the injection room should be kept at warm temperature. Patients are also advised to minimize muscle activity 24 hours before image acquisition to avoid increased muscular FDG uptake.

FDG is mostly excreted by the kidneys, and unlike glucose is not reabsorbed. Good hydration is recommended before FDG administration to improve target-to-background ratios. Patients are advised to urinate prior to ^{18}F-FDG PET/CT or ^{68}Ga-DOTA PET/CT acquisition and frequently afterwards. This limits artifact from renal excretion and decreases bladder radiation exposure.

Standard imaging extends from the skull base to the upper thighs. For head and neck studies the arms are placed down by the patient's side. This differs from other indications for which the patient's arms are usually raised. This reduces artifact on CT and attenuation correction artifact on PET imaging in the regions of interest. Patient motion during image acquisition can lead to misregistration artifact and should be recorded by the technologist (Fig. 1).

Attenuation Correction Artifacts

There are several artifacts that are unique to PET/CT, most of which result from the CT attenuation correction protocol. They most commonly relate to over or under correction. SUV values can be increased or decreased depending on whether the corresponding CT attenuation has been increased or decreased, respectively.

Dental Prosthetics, Metallic Implants and Ports

Dental prosthetics, metallic implants or chemotherapy ports represent common artifacts in PET/CT imaging of the head and neck. In the presence of these high density materials, standardized uptake value (SUV) measurement is compromised.

High photon absorption from high density material produces streak artifacts on CT images. This disturbs the normal attenuation distribution and correspondingly increases the PET attenuation coefficient. This leads to over-attenuation of PET images and results in falsely increased FDG uptake in the region.[19] Algorithms are available for the correction of CT dental artifacts by means of increasing or decreasing the Hounsfield units in the regions with under or overestimated values.[20,21]

Adequate PET/CT interpretation can be difficult in the presence of metal induced artifacts. The appearance of increased radiotracer uptake can mimic a focal mass within the oral cavity or if identified surrounding a metallic prosthesis or chemotherapy port can be mistaken for infection.[22] Retained radiotracer within the port or central venous catheter can also mimic artifact and injection via a peripheral intravenous line is therefore preferred.[23]

Alternatively, in patients with head and neck tumors involving the tonsils or oral cavity, attenuation overcorrection can mean that even a large tumor may be difficult to appreciate.[19] Metal-induced artifacts are only demonstrated on attenuation corrected PET images. In order to avoid this interpretation pitfall, it is necessary to review the non-attenuation corrected PET images[24-27] (Fig. 1).

Intravenous Contrast Medium

Some institutions advocate a contrast enhanced CT for attenuation correction. This has the advantage of allowing a single examination to stage a tumor and plan treatment.[28] Using post contrast CT imaging for attenuation correction can lead to overcorrection of PET data due to dense contrast material within vascular structures and can lead to clinically significant abnormalities being missed if they are located in the vicinity of contrast artifact.[29] Less commonly, it can lead to apparent focal FDG uptake mimicking a mass or abnormal lymph node.[30]

Calcified Lymph Nodes

Calcification of the mediastinal lymph nodes is relatively common. The markedly increased density of these nodes can lead to apparent increased FDG uptake potentially mimicking mediastinal lymphadenopathy. This can alter patient management, particularly in the setting of lung cancer as it can lead to nonsurgical management if the non contrast CT is not adequately interrogated. In the setting of head and neck SCC, this artifact could lead to an incorrect nodal staging. This pitfall is relatively easy to avoid by assessing the non-attenuation corrected PET and non contrast CT images.[23]

Physiological Variants

Muscular Uptake

FDG uptake in the muscles of the head and neck is a common physiological finding that may hamper adequate PET/CT interpretation. Several muscles within or adjacent to the oral cavity, oropharynx and hypopharynx demonstrate physiologic FDG uptake. These include the muscles of the floor of the mouth, the pterygoid muscles, the tongue and

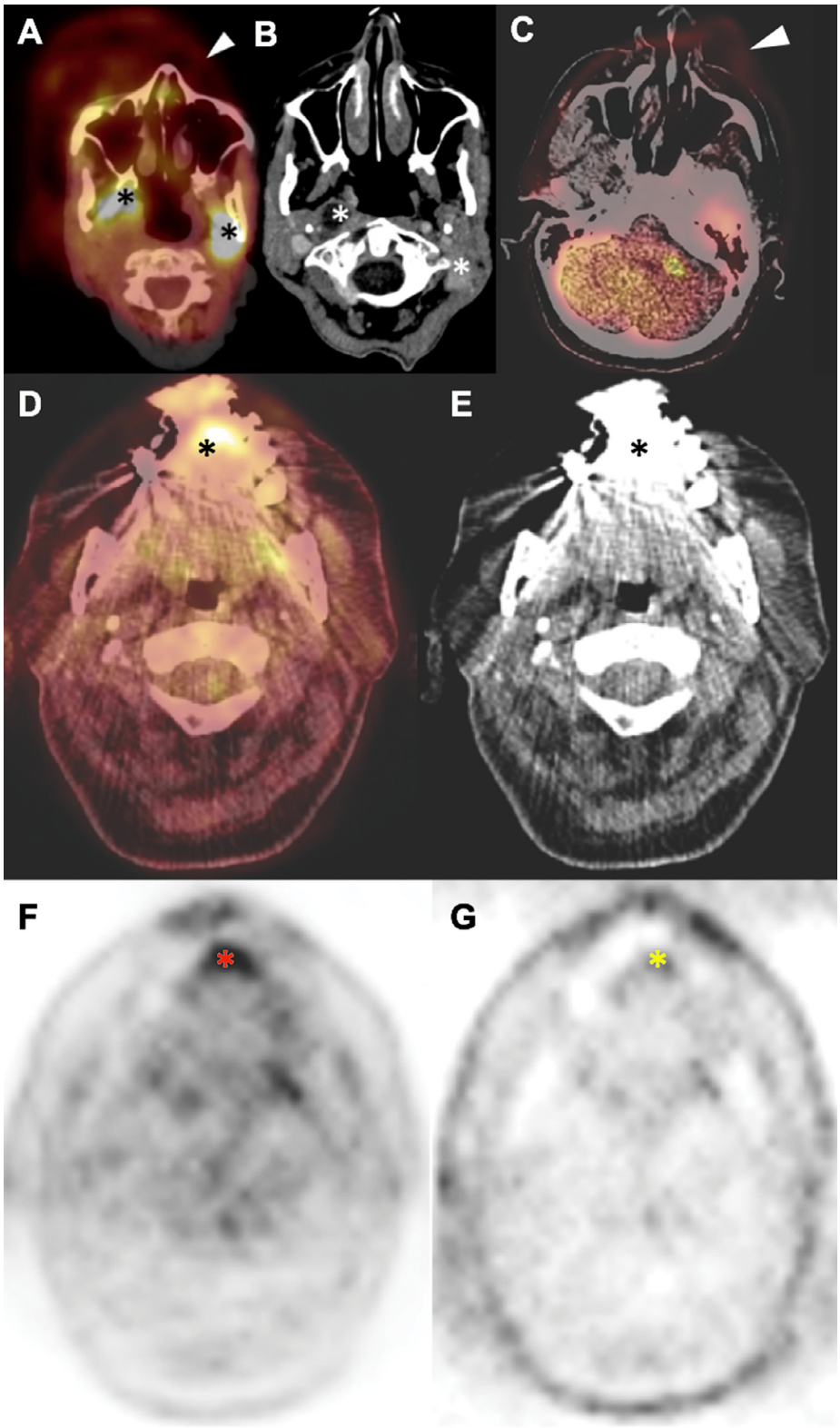

Figure 1 **Patient 1 (A and B): (A)** Axial ^{18}F-FDG PET/CT demonstrates misregistration artifact due to patient movement (white arrow). The FDG-avid lesions projected over the right sided pterygoid plates and left level II on ^{18}F-FDG PET/CT (black asterisks) are actually located within the right masticator space and the posterior triangle of the left side of the neck on CT **(B)** (white asterisks). **Patient 2: (C)** ^{18}F-FDG PET/CT with misregistration artifact due to movement of the patient's head (white arrow). **Patient 3 (D-G): (D)** ^{18}F-FDG PET/CT with apparent increased radiotracer uptake within the floor of the mouth. **(E)** Axial non contrast CT demonstrates beam hardening artifact from dental prosthetics. **(F)** ^{18}F-FDG PET with attenuation correction demonstrates apparent increased uptake corresponding with the area of beam hardening artifact on CT (asterisk) but this is not visible on the non-attenuation corrected image **(G)** consistent with attenuation correction artifact (asterisk).

cricopharyngeus.[29,31] Asymmetric uptake may mimic a malignant tumor or lymph node but the CT images can be assessed for a corresponding mass.

Talking during the FDG uptake phase can result in increased uptake within the muscles of phonation and vocal cords[31] (Fig. 2). Increased metabolic activity can also be detected in the lingual region and masseter muscles.[29,31-33] Excessive eye movements prior to image acquisition leads to increased uptake within the extraocular muscles[34] (Fig. 2). Coughing results in increased uptake within the pharyngeal constrictor muscles and vocal cords (Fig. 2). A unilateral vocal cord palsy can lead to altered physiology within the contralateral vocal cord and resultant increased FDG uptake.[35] Each of these appearances can mimic malignancy but this can usually be easily clarified on the non contrast CT.

Diffuse FDG uptake within the skeletal muscles is caused by strenuous patient exercise prior to image acquisition[32] (Fig. 2). Increased physiological uptake in the cervical and paraspinal muscles occurs because of anxiety related muscle contraction (Fig. 2). This can mimic metastatic lymphadenopathy or obscure underlying malignant adenopathy resulting in either a false positive or false negative result.[29,32,33,36,37] Physiological activity in the muscles is usually presented as linear FDG uptake with further characterization on CT images helpful in differentiation from abnormal lymph nodes.[29,36] In order to reduce contraction-induced muscle uptake in anxious patients some authors suggest administration of benzodiazepine in selected patients.[38] As outlined above, insulin administration prior to PET/CT acquisition induces diffuse FDG uptake in skeletal muscles and consequently compromises interpretation of the study.[39]

Lymphoid Tissue of Waldeyer's Ring

Symmetric FDG accumulation within lymphoid tissue is often seen in younger patients and is a normal variant. It can also be due to benign conditions such as infection, inflammation, or granulomatous processes (Fig. 3). These benign conditions may also present as focal FDG uptake, leading to false positive interpretation of PET/CT[29,33,40-43] (Fig. 3). While there is variation in FDG uptake in normal tonsilar tissue, it is usually relatively symmetric with only small differences in metabolic activity between the right and left sides. Because of this strong side to side correlation, an SUVmax ratio is probably more robust than differences in absolute SUVmax values.[44] One single center study of 25 patients suggests an asymmetry ratio of $\geq$1.6 as being highly suspicious for malignancy, with a reported sensitivity of 62% and specificity of 100%.[45]

Brown Fat Uptake

There are two different types of adipose tissue, white adipose tissue (WAT) and brown adipose tissue (BAT). WAT serves as a thermal insulator and a provider of energy storage but it also has a complex metabolic role. In contrast, the main role of BAT is in thermoregulation – it produces heat in response to cold exposure and after food intake – thermogenesis.[46-49]

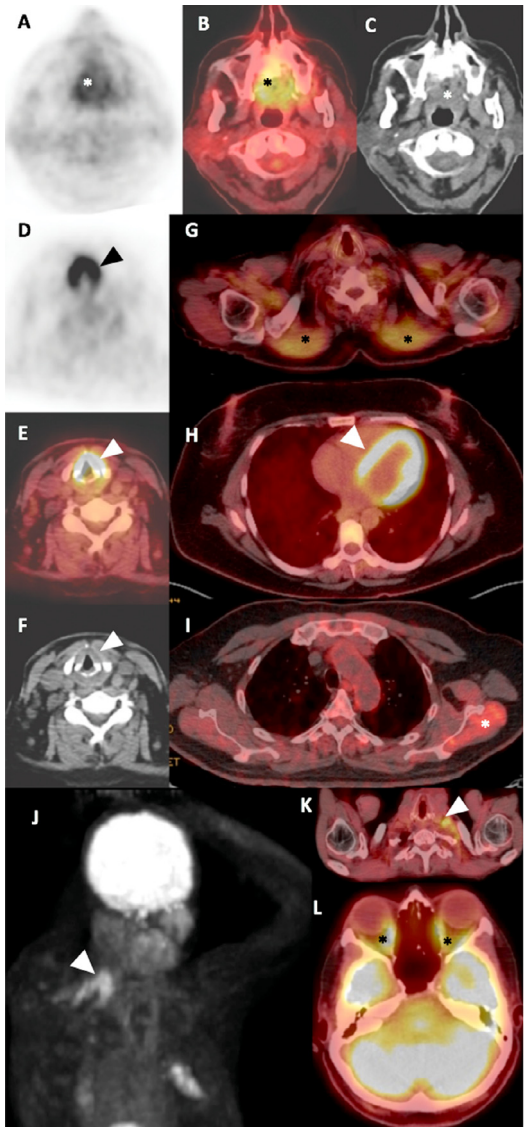

Figure 2 **Patient 4 (A-C): (A)** Axial ^{18}F-FDG PET, **(B)** axial ^{18}F-FDG PET/CT and **(C)** axial CT demonstrate increased uptake within the musculature of the tongue without a corresponding mass (asterisks). This is due to talking during the radiotracer uptake phase. **Patient 5 (D-F): (D)** Axial ^{18}F-FDG PET, **(E)** axial ^{18}F-FDG PET/CT and **(F)** axial CT demonstrate increased uptake within the vocal cords without a corresponding mass (arrows) in keeping with physiological uptake due to phonation. **Patient 6: (G)** Axial ^{18}F-FDG PET/CT demonstrates increased uptake within the trapezius muscles bilaterally in an anxious patient (asterisks). **Patient 7: (H)** Axial ^{18}F-FDG PET/CT demonstrates normal physiological myocardial FDG uptake (arrow). **Patient 8: (I)** Axial ^{18}F-FDG PET/CT demonstrates increased FDG uptake within the left infraspinatus muscle (white asterisk) after a patient was required to drive between hospitals during the uptake phase due to a technical malfunction with the only available on-site PET/CT scanner. **Patients 9 and 10: (J and K)** Maximum intensity projection (MIP) and axial ^{18}F-FDG PET/CT images demonstrate increased physiological uptake within the sternocleidomastoid muscles (white arrows). The MIP images demonstrate linear uptake corresponding with the two heads of sternocleidomastoid. **Patient 11: (L)** Axial ^{18}F-FDG PET/CT demonstrates normal physiological uptake within the extraocular muscles (black asterisks).

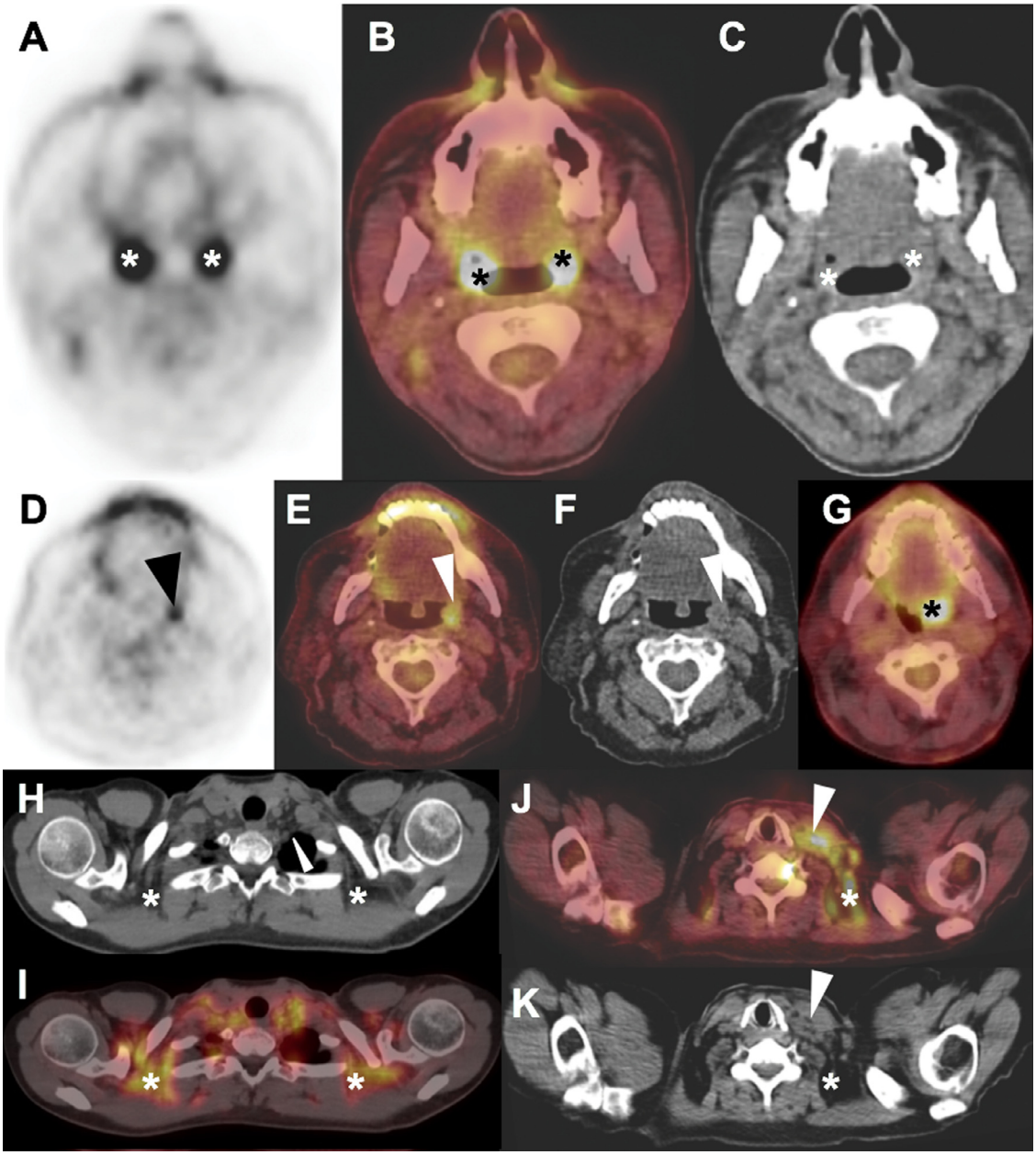

Figure 3 **Patient 12: (A-C): (A)** Axial ^{18}F-FDG PET, **(B)** axial ^{18}F-FDG PET/CT and **(C)** axial non contrast CT demonstrate increased radiotracer uptake within the palatine tonsils (asterisks) (SUVmax 9.5 on the right and SUVmax 10.2 on the left) secondary to biopsy proven chronic tonsillitis. **Patient 13: (D-F): (D)** Axial ^{18}F-FDG PET and **(E)** axial ^{18}F-FDG PET/CT demonstrate asymmetrically increased FDG uptake within the left palatine tonsil (arrows) (SUVmax 4.7). Biopsy confirmed non-Hodgkin's lymphoma within this tonsil. Axial non contrast CT demonstrates that the abnormal tonsil has a nodular appearance (arrow) compared to the contralateral side. **Patient 14: (G)** Axial ^{18}F-FDG PET/CT in another patient demonstrates avid FDG uptake within the left palatine tonsil (asterisk) post right-sided tonsillectomy. Both palatine tonsils had been markedly FDG-avid prior to tonsillectomy raising the possibility of malignancy. Postsurgical pathology demonstrated actinomycosis infection. **Patient 15: (H and I): (H)** Axial non contrast CT and **(I)** ^{18}F-FDG PET/CT demonstrate normal physiological FDG uptake within brown fat (asterisks). **Patient 16: (J and K): (J)** Axial ^{18}F-FDG PET/CT and **(K)** axial non contrast CT demonstrate FDG-avid soft tissue within the left supraclavicular fossa in keeping with the patient's known diagnosis of Hodgkin's lymphoma (arrows). Increased physiological FDG uptake within the adjacent brown fat (asterisks) makes this area of abnormality difficult to visualise.

Thermogenesis occurs due to a specific mitochondrial uncoupling protein (UCP-1). Uncoupling of oxidative phosphorylation within mitochondria generates heat.[50,51]

FDG uptake in BAT has been reported with an incidence of 2.5%-4%.[49,52,53] Hypermetabolic BAT is more common in women, in children and young patients and in those with a low body mass index. It also increases in cold weather.[49,54,55] Since BAT is innervated by the sympathetic nervous system, glucose accumulation within brown fat is increased by sympathetic stimulation.[56] Following rapid

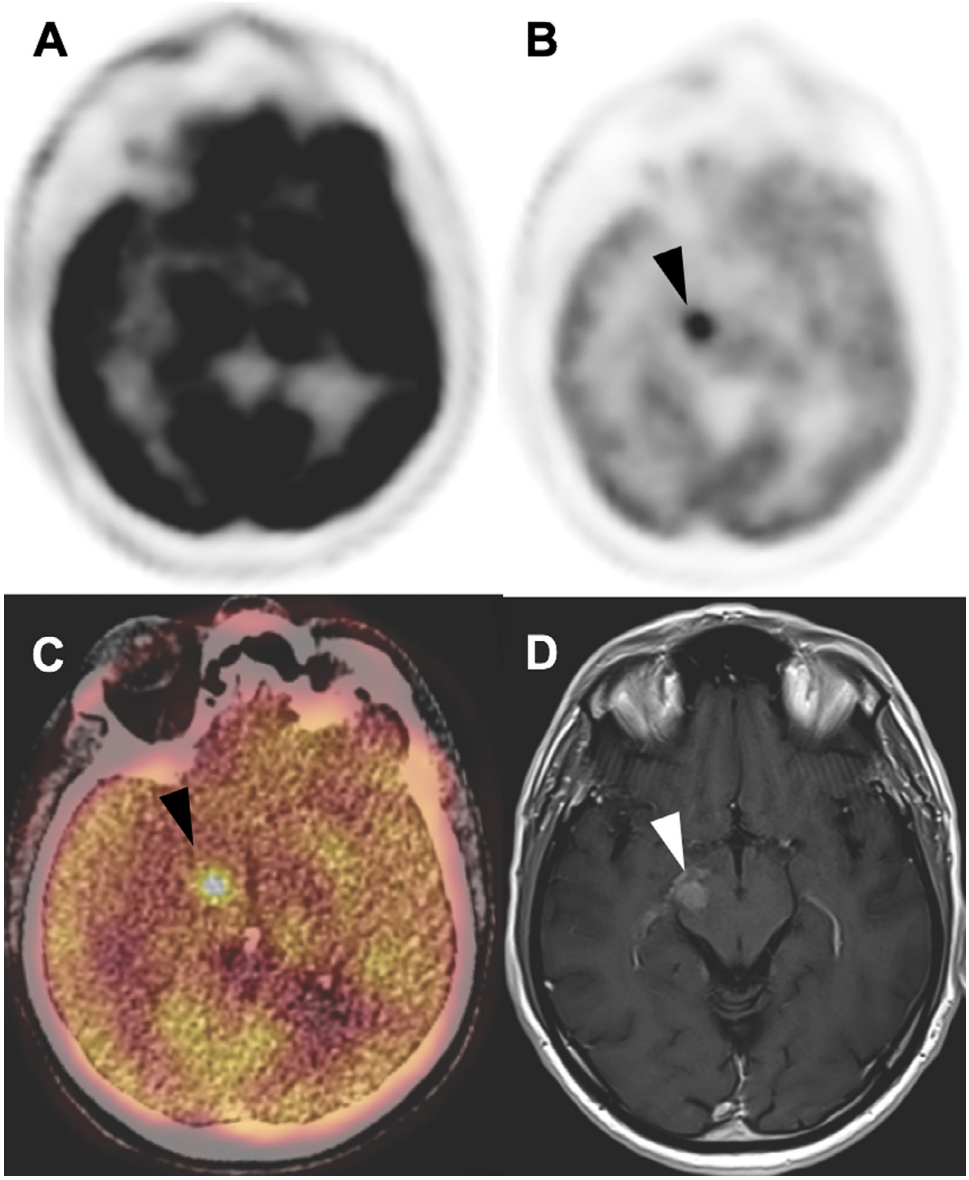

Figure 4 Patient 17: **(A-D): (A)** Axial ^{18}F-FDG PET demonstrates normal physiological uptake within the brain. The avid physiological uptake may obscure an underlying intracranial mass lesion. **(B)** Axial ^{18}F-FDG PET and **(C)** Axial ^{18}F-FDG PET/CT with appropriate windowing. It is possible to visualize an FDG-avid lesion within the right side of the midbrain (arrows). **(D)** Postcontrast T1-weighted MRI confirmed an enhancing lesion within the right crus cerebri. This patient also had a second lesion within the posterior fossa (not shown here). Biopsy confirmed intracranial non-Hodgkin's lymphoma.

weight loss, cancer patients have a lower body mass index (BMI) and are more prone to cold stress. The stimulation of the sympathetic nervous system in these patients induces thermogenesis. Increased BAT glucose metabolism can be reduced by adequate patient warming prior to FDG injection. In addition, drug administration with beta blockers (including propranolol), diazepam and fentanyl have been reported to reduce BAT uptake.[54,57,58]

Increased metabolic activity in BAT is visualized as symmetric, bilateral increased FDG uptake within the supraclavicular fossae, within the neck, the thorax, axillae and the paraspinal and retroperitoneal fat[49] (Fig. 3). Due to brown fat activation, nodal involvement may be difficult to appreciate on PET imaging in patients with primary tumors of the head and neck or lymphoma. The corresponding CT images can aid differentiation between physiological and pathological FDG uptake where increased BAT activity and nodal pathology are both present (Fig. 3).

Pitfall – Windowing Error

Normal physiological uptake within the grey matter of the brain is quite marked and can obscure intracranial pathology including space occupying lesions. Metastases are the most common intracranial mass lesions but the differential includes primary gliomas or lymphoma. These lesions can present as focal areas of increased or decreased intracranial FDG uptake. Adequate windowing when interpreting images of the brain or other areas of high physiological FDG uptake is required to prevent a false negative result[59] (Fig. 4).

Oral Cavity, Pharynx and Larynx

SCC commonly arises from the oral cavity, pharynx or larynx and constitutes 90% of cases of head and neck cancer.[60] SCC of the oral cavity or pharynx has an overall 5-year survival of 63% but life expectancy is significantly shortened in the presence of positive lymph node involvement.[61] HNSCC is staged by the 2018 AJCC/UICC tumor classification system and it is important that the reporting physician has these criteria to hand when reporting head and neck cancer PET studies.[62,63] This enhances the imaging report and ensures critical information is included to allow accurate T, N and M staging.

Imaging Pitfalls and How to Avoid Them

Pitfall - Local Tumor Staging

^{18}F-FDG PET/CT is highly sensitive in the detection of primary head and neck cancers but is limited by its poor spatial resolution when it comes to accurately staging local invasion.[64-66] Initial imaging of the primary site should be performed with contrast enhanced CT and/or MRI, with certain tumor locations better served by one or other of these modalities. For example, MR is preferred for nasopharyngeal SCC because of its ability to detect skull base involvement and for oral cavity tumors due to its ability to detect extrinsic tongue muscle invasion[67] (Fig. 5).

Pitfall - Bone marrow infiltration

Assessing the presence and extent of bony mandibular involvement is essential for surgical planning. Metabolic activity within the mandible tends to overestimate the extent of tumor due to a combination of partial volume effect and misregistration artifact. The CT component of PET/CT has a greater sensitivity and specificity for mandibular involvement than PET alone.[68] It can be used to detect cortical bone erosion that may not be visible on MR. MR on the other hand is useful in the detection of bone marrow infiltration. Combining information from CT, PET and MR results in the greatest accuracy when assessing for the presence or extent of mandibular involvement[69] (Fig. 5).

Pitfall - Perineural Spread

Some head and neck tumors are able to use local cranial nerve branches as a conduit for tumor growth. This perineural spread is most classically associated with adenoid cystic carcinoma but as this tumor is relatively rare among head and neck malignancies, SCC is the most commonly implicated tumor. Perineural spread infers a poor prognosis even when asymptomatic. It is often not recognized at the time of surgery and can occur in the absence of local lymphadenopathy or distant metastatic disease. While MRI is the modality of choice when it comes to assessing perineural spread it can also be visualized on ^{18}F-FDG PET/CT as asymmetric linear or curvilinear hypermetabolic activity.[70] If suspected on ^{18}F-FDG PET/CT, retrospective evaluation of the prior contrast enhanced MR should be performed to improve accuracy[71] (Fig. 6).

Pitfall – Vocal Cord Palsy

Injury to the recurrent laryngeal or vagus nerve (proximal to the branch point of the recurrent laryngeal nerve) along their course from the brainstem to the aortic arch on the left side and subclavian artery on the right side, can result in a vocal cord palsy (VCP). Up to 40% of unilateral cases are asymptomatic and the PET/CT reader may be the first to report the finding.[72,73] Iatrogenic injury is the most common cause, accounting for 37% of cases.[74] Another common cause is malignancy remote from the larynx accounting for 14% of cases.[75] For this reason, ^{18}F-FDG PET/CT imaging must be reviewed thoroughly from the skull base to the right subclavian artery and aortic arch to assess for a mass lesion along the course of the ipsilateral vagus or recurrent laryngeal nerves. 20% of cases are idiopathic and 6% due to trauma at intubation.[75]

The most specific imaging characteristics of a vocal cord palsy are; enlargement of the ipsilateral laryngeal ventricle, medialisation and thickening of the ipsilateral aryepiglottic fold and widening of the ipsilateral piriform sinus. In combination, these findings are reliable for the detection of VCP, with at least 2 of the 3 findings present in all 31 patients in one small study.[76] Another helpful finding is the vocal cord "sail sign" (Fig. 6). This appearance is due to a combination of medialisation of the posterior vocal cord secondary to anteromedial displacement of the ipsilateral arytenoid cartilage and distension of the ipsilateral laryngeal ventricle due to muscular atrophy.[77,78]

Unilateral VCP can result in compensatory increased uptake within the contralateral vocal cord on ^{18}F-FDG PET/CT, potentially mimicking a vocal cord mass lesion. The corresponding CT imaging should be reviewed to assess for irregularity of the contralateral vocal cord or soft tissue within the immediately adjacent paraglottic fat.[35] Laryngoscopy can confirm vocal cord paralysis and assess for a contralateral vocal cord mass.

Thyroid Gland

Physiological and Benign Variations in FDG Uptake

The thyroid gland usually demonstrates homogeneous low FDG uptake, but may have a variable appearance.[40,79-82] On ^{18}F-FDG PET/CT, incidental uptake within the thyroid gland can appear as diffuse, focal or a combination - diffuse and focal. According to several studies, 1.2%–4.3% of patients have incidental thyroid abnormalities detected at ^{18}F-FDG PET/CT,[80,83-88] while some authors report an even higher prevalence of thyroid incidentalomas of 8.4%.[79]

Symmetric and diffuse thyroid uptake is usually benign in nature. It has a number of potential etiologies including diffuse or multinodular goiter, autoimmune Hashimoto thyroiditis or Graves' disease[80,89-98] (Fig. 7). There are several reports of diffusely increased thyroid uptake in hypothyroid patients, with or without thyroid hormone replacement.[80,93,96] Asymmetric FDG uptake in the thyroid

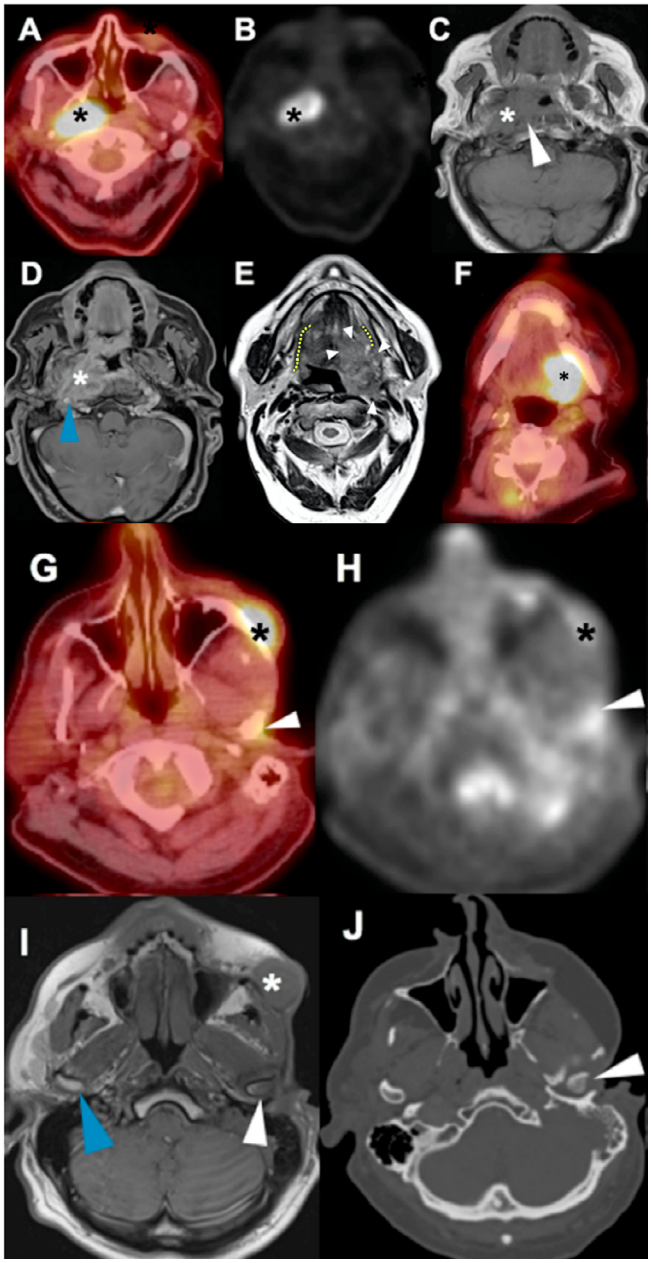

Figure 5 **Patient 18: (A-D): (A)** Axial ^{18}F-FDG PET/CT and **(B)** axial ^{18}F-FDG PET demonstrate an FDG-avid mass arising from the nasopharynx and extending into the adjacent masticator space in keeping with locally invasive nasopharyngeal carcinoma (asterisks). It is not possible to accurately assess the surrounding structures on ^{18}F-FDG PET/CT in order to provide an accurate T-stage. **(C)** T1 weighted MR and **(D)** postcontrast MR demonstrate that the mass (asterisk) invades the skull base (white arrow) and surrounds the right internal carotid artery (blue arrows) in keeping with a T4 tumor. **Patient 19: (E and F): (E)** Axial T2 weighted MR demonstrates a mass arising from the musculature of the tongue (asterisk). The boundaries of the mass are delineated by white arrows. The normal right hyoglossus muscle is delineated by a blue dotted line on the contralateral side. The left hyoglossus muscle is delineated by an interrupted blue-dotted line as it is invaded by the mass in keeping with T4 staging. This mass was markedly avid on ^{18}F-FDG PET/CT **(F)** but it was not possible to discern the boundaries of local invasion (asterisk). This could potentially lead to an incorrect T-stage being applied. **Patient 20: (G-J): (G)** Axial ^{18}F-FDG PET/CT and **(H)** axial ^{18}F-FDG PET in a patient with recurrent SCC (asterisk). There is a subtle focus of increased uptake over the condyle of the left mandible which could represent a further focus of recurrent disease or treatment effect (white arrow). There was no associated cortical erosion on the accompanying CT imaging. **(I)** T1-weighted MR demonstrates corresponding low T1 signal within the condyle of the left mandible consistent with recurrent disease (white arrow). In contradistinction to this, radiation change is associated with increased T1 signal due to fat deposition within the bone marrow. Note the normal signal within the condyle of the right mandible (blue arrow). **(J)** Axial CT image 6 months later demonstrates cortical erosion of the condyle of the left mandible (white arrow). This was not present on earlier CT imaging.

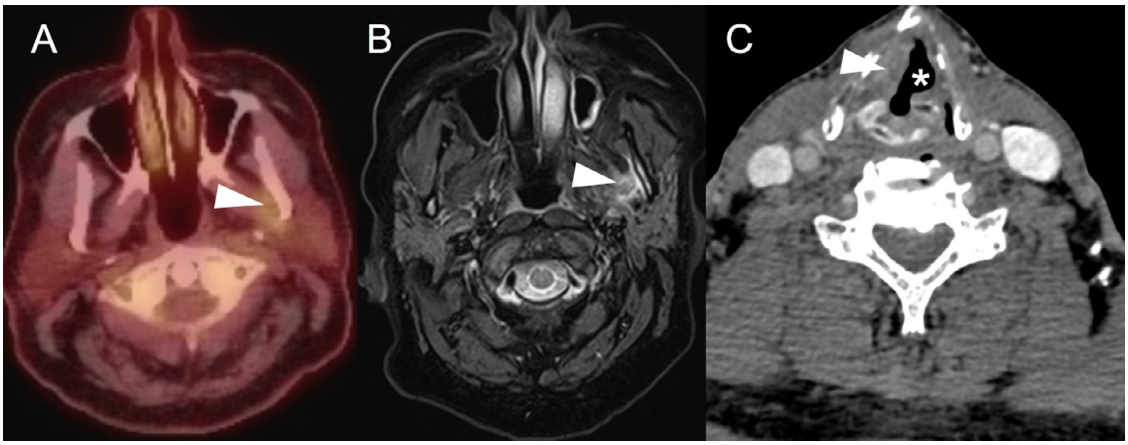

Figure 6 **Patient 21: (A and B): (A)** Axial ^{18}F-FDG PET/CT demonstrates subtle increased FDG uptake in the left masticator space (white arrow) in a patient with previously treated SCC. A corresponding focus of linear STIR high signal (white arrow) on MRI **(B)** is in keeping with perineural spread. **Patient 22: (C)** Axial contrast enhanced CT demonstrates a left-sided sail sign (asterisk) in keeping with a left-sided vocal cord palsy. This patient also has a mass on the right vocal cord (white arrow).

gland is non-specific. It may be a result of a benign thyroid nodules.[99]

Pitfall – The FDG-Avid Thyroid Nodule

Focal FDG uptake in thyroid gland may also represent malignancy. According to several studies, the risk of malignancy in thyroid incidentalomas ranges from 23.2% to 50%.[79,80,85-87] The risk of cancer has been reported to be as high as 6.4% in patients with diffuse or bilateral thyroid uptake but increases further to 30.9% in focal and unilateral thyroid uptake.[79] The rate of malignancy associated with focal thyroid uptake on the ^{18}F-FDG PET/CT differs among studies with a wide range reported of between 14 % and 100%.[79,80,83,84,86-88,100-110] Focal uptake on ^{18}F-FDG PET/CT may also be falsely interpreted as metastatic lymphadenopathy, particularly at the lower cervical level. This can be further assessed on the corresponding CT images.

In patients with focal thyroid uptake, ultrasonography is usually performed and thyroid nodules are classified according to the ACR TI-RADS criteria for thyroid malignancy.[111] However, the TI-RADS scoring system does not take into account features identified on ^{18}F-FDG PET/CT. This is important as FDG avidity within a thyroid nodule increases the risk of malignancy and fine needle aspiration may be required for nodules classified as low risk by ACR TI-RADS[112] (Table 1). FDG avidity may in future supplement the ACR TI-RADS criteria by adding points to a nodule with hypermetabolic activity (Fig. 7).

Pitfall – Metastatic Thyroid Carcinoma

^{18}F-FDG PET/CT is a useful tool to detect metastases in differentiated thyroid cancer (DTC).[113] As DTC cells dedifferentiate, their FDG uptake tends to increase and their radioiodine uptake decreases – this is known as the flip-flop

Table 1 TI-RADS Scoring System, Risk of Malignancy and Management Recommendations

TI-RADS Category	Score	Risk of Malignancy Based on Sonographic Features Only (%)	Recommendation Based on Sonographic Features Only	Risk of Malignancy If Also Focally FDG Avid on ^{18}F-FDG PET/CT
TR1	0	Benign (<2%)	No FNA	0%*
TR2	2	Not suspicious (<2%)	No FNA	16.7%*
TR3	3	Mildly Suspicious (2.1-5%)	FNA if >2.5 cm US follow-up at 1, 3 and 5 years if >1.5 cm	13.2%
TR4	4-6	Moderately suspicious (5.1-20%)	FNA if >1.5 cm US follow-up at 1, 2, 3 and 5 years if >1 cm	23.7%
TR5	>6	Highly suspicious (20%)	FNA if >1 cm US follow-up annually for 5 years if >0.5 cm	68.1%

ACR TI-RADS scoring system, associated nodule risk and recommendation based on sonographic features alone. The last column demonstrates the change in risk profile for each TI-RADS category if the nodule is FDG-avid on ^{18}F-FDG PET/CT.[112]

*Low numbers studied in both TR1 (n = 1) and TR2 (n = 6) nodules. Results should be interpreted with caution; US, ultrasound.

pattern.[114-116] ^{18}F-FDG PET/CT is therefore most useful in the absence of radioiodine uptake with a sensitivity of 94% for metastatic disease in this setting[117] (Fig. 7). Metastatic medullary thyroid carcinoma (MTC) demonstrates poor FDG uptake. It is therefore difficult to detect at ^{18}F-FDG PET/CT, particularly when the serum calcitonin is less than 1000pg/ml when the pooled detection rate drops from 75% to 20-36.8%[118-121] (Fig. 7).

Salivary Glands

Physiologic or Benign Variations in FDG Uptake

Salivary glands physiologically accumulate FDG and eliminate the tracer via saliva[122] (Figure 8). In most cases, they demonstrate bilateral mild FDG uptake, but they may also demonstrate no uptake. The usual pattern of physiological uptake in salivary glands is diffuse and symmetric and detection of focal and heterogeneous FDG uptake can indicate malignancy. In contrast, symmetric uptake has been also reported in malignancy particularly in extranodal Non-Hodgkin's lymphoma and SCC.[29-33]

As increased salivary gland FDG uptake can be detected in both benign and malignant conditions, interpretation of ^{18}F-FDG PET/CT scans can be challenging. Benign conditions of the salivary glands associated with increased FDG uptake include benign tumors (Warthin's tumors, pleomorphic adenomata and infectious or inflammatory diseases such as tuberculous infection, obstructive sialoadenitis, calculosis, sarcoidosis or post-irradiation sialoadenitis[123-125] (Fig. 8).

Asymmetric FDG uptake can be detected in a remaining submandibular gland secondary to contralateral salivary gland resection, or in patients following unilateral gland external radiation treatment[29,33] (Fig. 8). This can be misinterpreted as metastatic nodal involvement at levels IB/II.[41,126,127]

Pitfall – The Malignant Salivary Gland Tumor

Malignant tumors of the salivary glands are rare accounting for only 3% of all head and neck neoplasms. In most cases, they originate from the parotid gland although around 75% of parotid gland tumors are benign in nature.[128] Malignant etiologies of increased metabolic activity in the salivary glands include metastatic tumours or primary parotid non-Hodgkin's lymphoma.[129] High-grade malignant tumours of the salivary glands usually present with high FDG uptake, in contrast to low-grade tumours, which show relatively low FDG uptake. As increased FDG activity within the salivary glands can mimic or hide tumours, differentiation between normal physiologic FDG uptake and pathological activity can be difficult.[82,130-132] Further diagnostics with ultrasound guided biopsy or MRI may also be required for a definitive diagnosis.[29,33,133] A study by Kendi et al concluded that PET/CT parameters cannot adequately differentiate benign, malignant or metastatic parotid tumours[134] (Fig. 8).

Lymphoid Structures and Nodal Staging of HNSCC

The risk factors classically associated with HNSCC are tobacco and alcohol. However, more recently, another subgroup of patients with a different risk factor profile has emerged – patients with HPV associated SCC of the oropharynx.[135] HPV positive oropharyngeal SCC is associated with a younger age at presentation, male gender and higher socioeconomic status and education.[136-139] It has increased in incidence by 2.7% in men and 0.8% in women each year from 1999 to 2015 and is now associated with 34% of cases of oropharyngeal SCC in Caucasians.[140,141] It has a significantly better prognosis than HPV negative oropharyngeal SCC despite a predisposition for early and extensive nodal metastases.[142,143]

The most recent AJCC/UICC guidelines have separated oropharyngeal cancers into these two separate groups, those that are associated with HPV infection (p16 positive) and those that are not (p16 negative) with separate nodal staging algorithms for each. This has the potential to cause confusion as the HPV status of the tumor may not be known at the time of image interpretation.[144]

Difficulty detecting a primary lesion on ^{18}F-FDG PET/CT can occur when the tumor is small or if it arises within a structure with high metabolic activity such as the lingual or palatine tonsils.[145,146] Careful evaluation of the CT images for signs of malignancy is necessary.[33,40,147] MR can be used as an adjunct when the primary lesion is not identified.[144]

Pitfall – Non-FDG–Avid Lymph Nodes and HPV Status

HPV associated oropharyngeal SCC is strongly associated with cystic lymphadenopathy.[148] These cystic lymph nodes infer a favorable prognosis over solid lymphadenopathy in this setting, however they may contain insufficient metabolically active tissue to demonstrate visible FDG uptake leading to false negative appearance at ^{18}F-FDG PET/CT (Fig. 9).[42,149] This can occur even in the setting of a metabolically active primary lesion. In this setting careful review of the CT component is necessary to identify abnormal but non avid nodes.

One of the hallmarks of a metastatic lymph node is an increase in short axis diameter resulting in a rounded appearance. However there is significant overlap in size between normal lymph nodes and those with malignant infiltration. A short axis diameter of greater than 10 mm is the most effective size criterion for malignant infiltration although a slightly larger cut-off of 11 mm is taken in level II. Groups of nodes are also considered suspicious, even if their short axis diameters are within these confines. Three or more lymph nodes together with short axis diameters of 8 mm or more (9 mm in level II) are considered suspicious. Loss of the central fatty hilum can also suggest malignant infiltration but this is best demonstrated on ultrasound.[150,151]

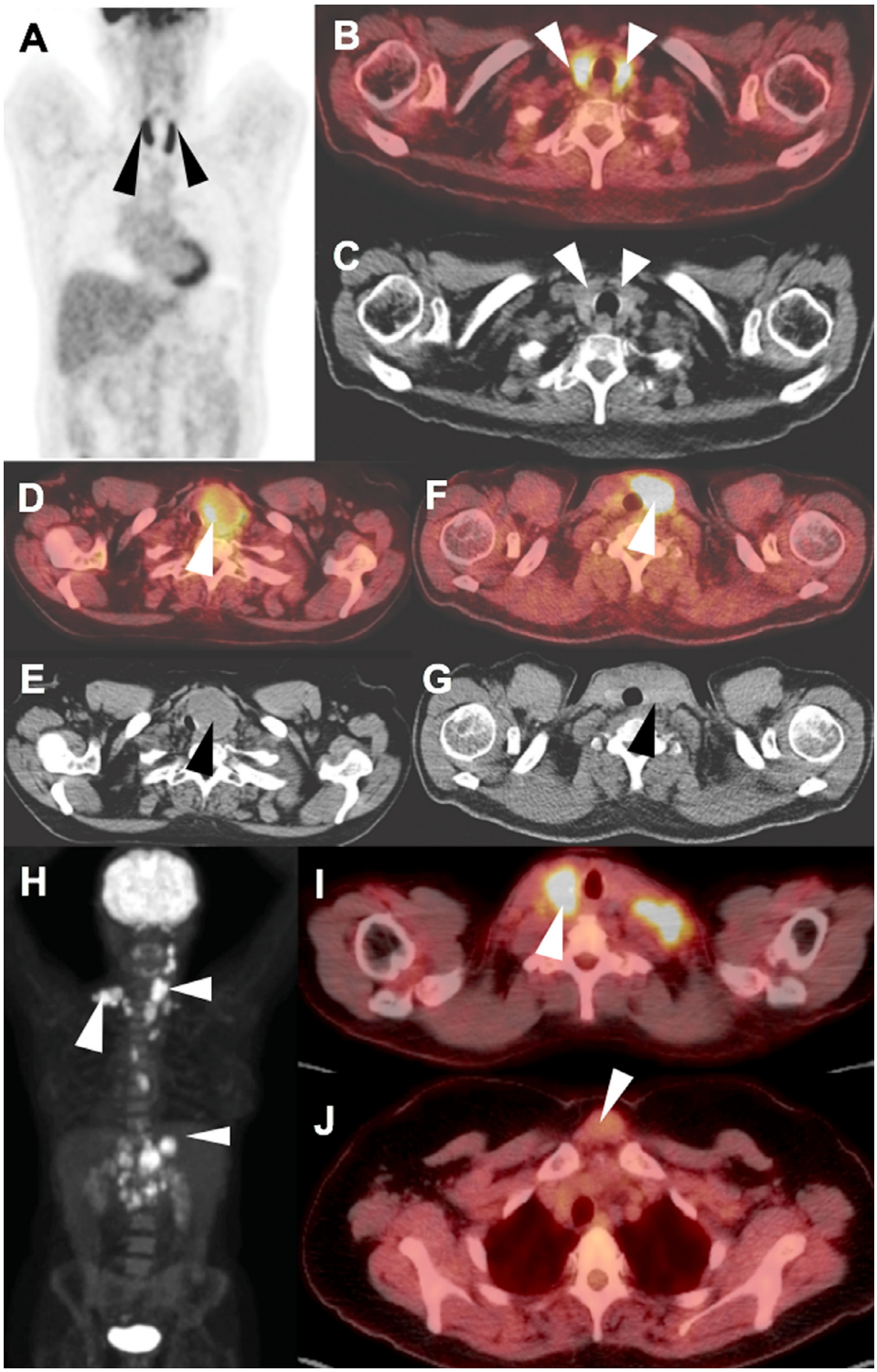

Figure 7 **Patient 23: (A-C): (A)** ^{18}F-FDG PET MIP image, **(B)** axial ^{18}F-FDG PET/CT and **(C)** axial CT in this patient with Hashimoto's thyroiditis. There is diffuse FDG uptake within the thyroid gland (arrows). **Patient 24: (D and E): (D)** Axial ^{18}F-FDG PET/CT demonstrates increased FDG uptake within the periphery of a left-sided thyroid nodule (white arrow). The corresponding CT image **(E)** demonstrates that the nodule is cystic (black arrow). This was proven to be benign. **Patient 25: (F and G): (F)** Axial ^{18}F-FDG PET/CT and **(G)** axial CT in this patient with lymphoma of the thyroid gland. There is marked FDG uptake and enlargement of the left thyroid lobe (arrows). **Patient 26: (H and I): (H)** ^{18}F-FDG PET MIP image demonstrating FDG-avid metastases within the neck, thorax and abdomen in this patient with metastatic papillary thyroid carcinoma (arrows). **(I)** Axial ^{18}F-FDG PET/CT demonstrates the primary lesion within the right lobe of the thyroid gland (white arrow). **Patient 27: (J)** Soft tissue nodule located at the sternal notch demonstrates faint FDG uptake consistent with metastatic medullary thyroid carcinoma (white arrow).

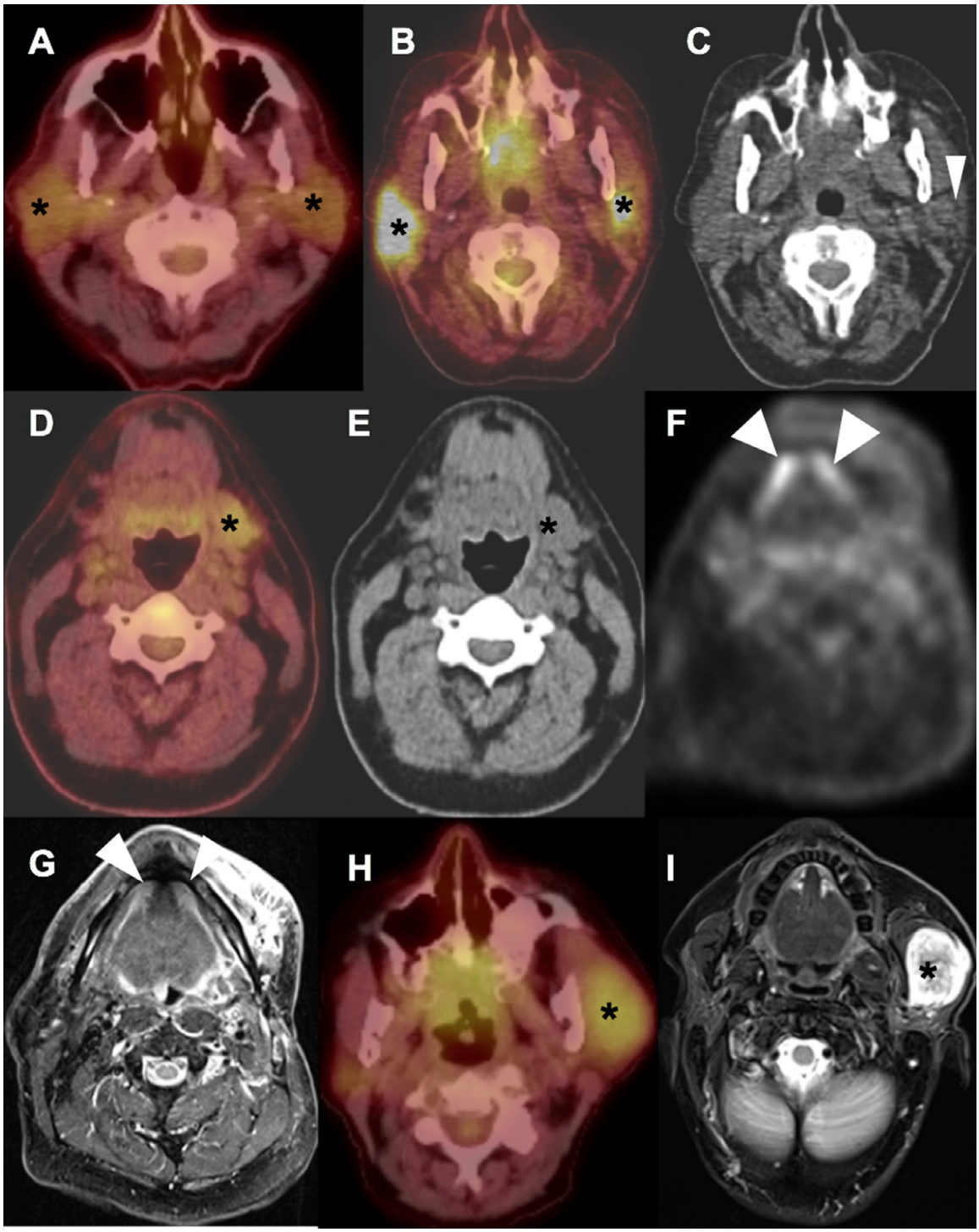

Figure 8 **Patient 28: (A)** Axial ^{18}F-FDG PET/CT demonstrates physiological low-grade uptake within the parotid glands (asterisks). **Patient 29: (B and C): (B)** Axial ^{18}F-FDG PET/CT and **(C)** axial CT in this patient with Sjogrens disease demonstrate intense FDG uptake within both parotid glands (asterisks), more marked on the right. There is partial fatty atrophy of the left parotid gland (white arrow) secondary to chronic inflammation. FDG uptake within the atrophied region is much less marked. **Patient 30: (D and E): (D)** Axial ^{18}F-FDG PET/CT demonstrates physiological uptake within the left submandibular gland (asterisk) and Axial CT **(E)** demonstrates absence of the right submandibular gland consistent with prior surgery. **Patient 31: (F and G): (F)** Axial ^{18}F-FDG PET in this patient with recurrent HNSCC demonstrates physiological uptake within the sublingual glands (arrows). **(G)** STIR weighted MR in the same patient demonstrates the normal appearance of the sublingual glands on MR (arrows). **Patient 32: (H and I): (H)** Axial ^{18}F-FDG PET/CT in this patient with a Warthin's tumor demonstrates increased FDG uptake and **(I)** STIR high signal within the superficial lobe of the left parotid gland (asterisks).

Table 2 A Summary Table of Each Variant or Pitfall With the Expected Imaging Appearances and a Suggested Solution or Management Plan to Optimize Patient Outcomes

Variant or pitfall	Finding	Solution
Attenuation correction artifact		
1. Dental prosthetics, metallic implants and ports	Streak artifact on CT image with falsely increased or decreased FDG uptake on PET images	Review the nonattenuation corrected PET images
2. Intravenous contrast medium	Dense contrast material in the vascular structures may result in attenuation overcorrection resulting in an artifactual increase in FDG uptake	Non contrast CT for attenuation correction is usually preferred for this reason
3. Calcified lymph nodes	Increased FDG uptake due to markedly increased lymph node density. This can mimic FDG-avid lymphadenopathy	Review the nonattenuation corrected PET and non contrast CT images
Physiological variants		
1. Muscular uptake (muscular activity during talking, chewing, prior exercise or prior insulin administration)	Increased FDG uptake may mimic a malignant tumor or nodal pathology	Review the CT images. The interpreter must be aware of normal patterns of FDG uptake
2. Waldeyer's ring	Increased FDG uptake may be due to infection, inflammation or granulomatous processes as well as due to malignant disease	Normal tonsils demonstrate symmetric FDG uptake with small differences in metabolic activity accepted. An SUVmax ratio of 1.6 is a useful cutoff for suggesting the possibility of malignancy but there is significant overlap with benign pathology
3. Brown fat tissue	Increased symmetric FDG uptake in the supraclavicular fossae, within the neck, thorax, axillae, and the paraspinal and retroperitoneal fat	Review corresponding CT images for corresponding fat attenuation. Corresponding soft tissue attenuation must be excluded as this is more in keeping with an FDG-avid mass
4. Windowing error	The brain demonstrates high physiological FDG uptake, particularly the cortex. This can obscure an underlying brain tumor or metastasis	Adequate windowing is essential to prevent a false negative result
	Masses that demonstrate avid radiotracer uptake for example, paragangliomas can appear larger than they actually are on PET/CT imaging	Adequate windowing allows for a more accurate measurement of the mass. The mass can also be measured on the non contrast CT.
Tumor detection, staging and follow-up		
1. Bone marrow involvement	Increased FDG uptake adjacent to or overlying bone	Combine CT, PET and MR imaging for the most accurate assessment. CT can demonstrate cortical erosion and MRI can demonstrate low bone marrow T1 signal in the setting of bone infiltration
2. Perineural spread	Asymmetric linear or curvilinear increase in FDG activity	Review the contrast enhanced and STIR MR images
3. Vocal cord palsy (VCP)	The sail sign on CT (Fig. 6) suggests a VCP. ^{18}F-FDG PET/CT often demonstrates compensatory increased FDG uptake within the contralateral vocal cord.	Review the corresponding CT images to exclude an underlying vocal cord mass. Laryngoscopy is required to confirm vocal cord paralysis. If VCP is confirmed, imaging along the course of the ipsilateral vagus and recurrent laryngeal nerves must be performed (from skull-base to aortic arch or right subclavian artery) to exclude an underlying mass.
4. Timing of post-treatment ^{18}F-FDG PET/CT imaging	Increased FDG uptake in recently irradiated tissues or following recent surgery may lead to a false positive	^{18}F-FDG PET/CT should be performed 12 weeks after radiotherapy or approximately 4-6 weeks following surgery

Table 2 (*Continued*)

Variant or pitfall	Finding	Solution
5. HPV associated SCC	Often associated with cystic lymphadenopathy which may not demonstrate increased FDG uptake	The accompanying CT imaging should be assessed for abnormal lymph nodes based on their size and appearance. Other modalities including US or MR imaging can also be assessed.
Thyroid gland		
FDG-avid thyroid nodules	FDG-avid thyroid nodules have a higher associated risk of malignant pathology for each given ACR TI-RADS TR category (Table 1)	Physicians must be aware of this increased risk. The management plan should be altered appropriately with a decreased threshold for FNA.
Metastatic differentiated thyroid cancer (DTC)	As DTC cells dedifferentiate, the FDG uptake increases and the radioiodine uptake decreases – the "flip-flop pattern"	^{18}F-FDG PET/CT is most useful in the absence of radioiodine uptake
Medullary thyroid cancer	Medullary thyroid cancer (MTC) can demonstrate poor FDG uptake	It may be very difficult to detect MTC metastases on ^{18}F-FDG PET/CT and other modalities including contrast enhanced CT may be required. Close comparison with prior imaging is essential
Salivary gland		
Benign vs malignant salivary gland lesions	Increased metabolic activity in the salivary glands can be detected in both benign and malignant conditions	Further diagnostics with US or MRI is required
Paragangliomas of the head and neck		
Appropriate follow-up	Up to 40% of paragangliomas of the head and neck are hereditary. Succinate dehydrogenase mutations are the most common	Genetic testing is recommended in all patients depending on local resources

Pitfall - Indeterminate Lymph Nodes

^{18}F-FDG PET/CT is more accurate (93%) than CT/MRI (86%) for nodal staging with reported sensitivities ranging from 86%-98% and specificities ranging from 88%-98.5%.[152-154] This increased sensitivity is due to the fact that ^{18}F-FDG PET/CT can detect hypermetabolic lymph nodes that are not enlarged and that are morphologically normal on CT and MR imaging. The SUVmax of malignant nodes can overlap with SUVmax values for reactive lymphadenopathy although values do tend to be significantly higher in the untreated patient.[155] Small lymph nodes may also be below the resolution of PET (4-6 mm) and therefore microscopic nodal disease may not be detected at ^{18}F-FDG PET/CT.[156] Ultrasound can be used to evaluate nodes that are indeterminate on PET/CT and guide biopsy if there is an abnormal US appearance.[157]

Metastatic Disease

Distant metastatic disease is relatively uncommon in HNSCC with an incidence ranging from 2% to 18%.[158] An additional 20%-30% develop metastases over the course of their disease. It most commonly affects the lungs followed by liver and bone. Metastatic disease implies a poor prognosis with a median survival of 10 months.[159] If metastatic disease is identified, unnecessary radical treatments can be avoided.[160] ^{18}F-FDG PET/CT has a negative predictive value of up to 99% for the evaluation of distant metastases at the time of diagnosis.[161]

Therapy Response

^{18}F-FDG PET/CT is a useful modality for assessing disease response and is recommended by the NCCN guidelines for therapy assessment following chemo-radiotherapy or radiotherapy alone.[16] It evaluates the cellular viability of the tumor and can therefore overcome the limitations of CT and MR which may demonstrate only nonspecific soft tissue changes associated with prior surgery or radiotherapy including edema, scarring and loss of fascial planes.[28] Novel chemotherapeutic agents can also be cytostatic as opposed to cytoreductive, with treatment response manifested by a reduction in tumor metabolism as opposed to a reduction in tumor size.

Benign Variations in FDG Uptake Post Treatment

There are four separate qualitative criteria for assessing treatment response; Deauville, Hopkins, Porceddu and NI-RADS, each of which have similar performance characteristics but

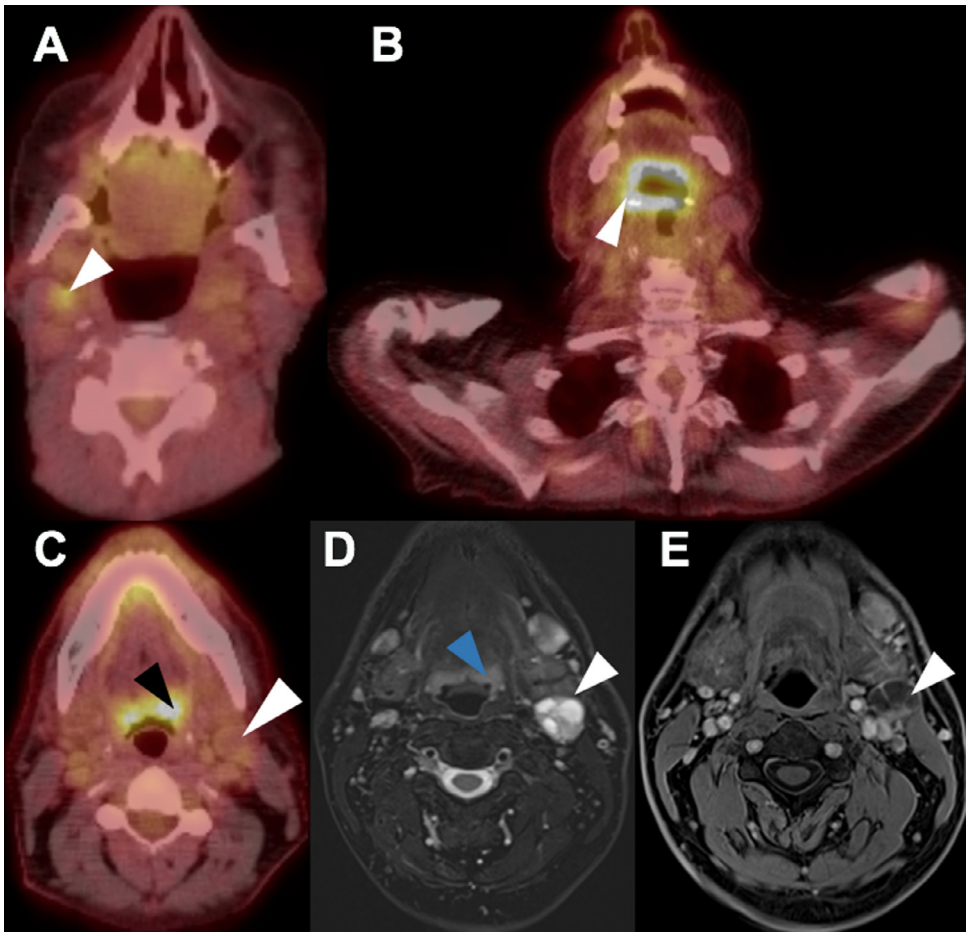

Figure 9 **Patient 33: (A)** Axial ^{18}F-FDG PET/CT demonstrates FDG uptake in a nodal metastasis in right level II in this patient with HNSCC (arrow). **Patient 34: (B)** Axial ^{18}F-FDG PET/CT demonstrates intense FDG uptake within the oral cavity and oropharynx (>2 × liver uptake) (arrow) in this patient with previously resected oropharyngeal SCC in keeping with disease recurrence (Deauville 5). **Patient 35: (C-E): (C)** Axial ^{18}F-FDG PET/CT in this patient with HPV associated oropharyngeal SCC demonstrates an enlarged left level II lymph node without corresponding FDG uptake (white arrow). There is also increased FDG uptake within the left lingual tonsil consistent with the primary lesion (black arrow). **(D)** Axial STIR weighted MRI and **(E)** axial postcontrast MRI demonstrate a peripherally enhancing cystic lymph node in the left level II (white arrows) consistent with a nodal metastasis. Its cystic nature accounts for the lack of increased FDG uptake. The left lingual tonsil has a normal appearance on STIR weighted MR (blue arrow).

the Deauville and Porceddu scales minimize the number of indeterminate cases while maintaining a high negative predictive value.[162]

The Deauville criteria are commonly used to predict regional control and remission of tumor after radiotherapy and allow for patients to be divided into two groups; responders and nonresponders.[163] This scale recognizes that FDG uptake on the post treatment study can represent benign disease and prevents misinterpretation of such findings as disease recurrence.[164]

Pitfall – Timing of Post Treatment ^{18}F-FDG PET/CT

The timing of post treatment ^{18}F-FDG PET/CT significantly influences its accuracy with guidelines suggesting a minimum delay of 12 weeks post radiotherapy or approximately 4-6 weeks postsurgery.[60] FDG uptake is increased in recently irradiated tissues and is more intense in tissues that received a higher radiation dose. The increased uptake can last for 12-16 months post radiotherapy.[165] Overlap in the SUVmax values demonstrated in radiation related inflammatory change and that of recurrent disease can lead to diagnostic uncertainty, particularly early on (less than 2 months post therapy).[166,167]

Tumor Recurrence

All patients with HNSCC are at risk of tumor recurrence or development of a second primary tumor. Recurrence tends to occur within the first three years following treatment. Delayed recurrence is more common in those with HPV positive HNSCC.[168]

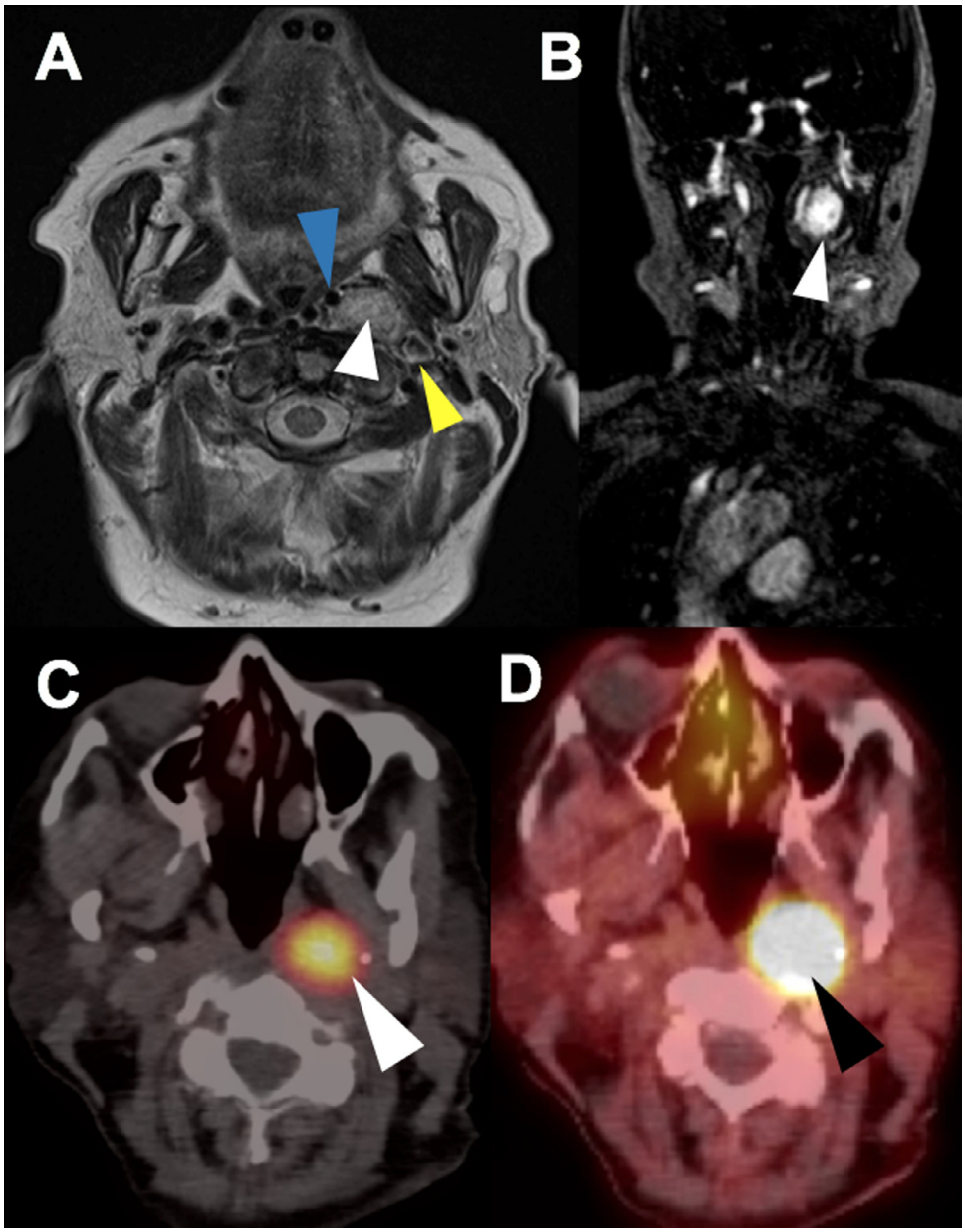

Figure 10 Patient 36: **(A-D): (A)** Axial T2-weighted MRI demonstrates a T2 high signal mass within the left side of the neck (white arrow). This mass splays the left internal carotid artery (blue arrow) and the left internal jugular vein (yellow arrow) in keeping with a carotid space mass, the differential for which includes a paraganglioma or vagal schwannoma. **(B)** Coronal MR angiography demonstrates that the left carotid space mass is hypervascular. **(C)** ^{68}Ga-DOTA PET/CT demonstrates a corresponding focus of increased radiotracer uptake consistent with a paraganglioma. **(D)** ^{68}Ga-DOTA PET/CT in the same patient with inadequate windowing. The lesion (black arrow) appears larger than it actually is due to intense radiotracer uptake.

The risk of recurrence is increased with higher stage tumours at diagnosis, positive surgical margins, perineural invasion and extracapsular lymph node spread. ^{18}F-FDG PET/CT is superior to CT, MRI and clinical examination for the detection of recurrent disease.[28,169] Its reported sensitivity in this setting ranges between 90% and 100% and specificity between 63% and 94%. The lower specificity is due to inflammatory uptake and tissue biopsy or a short interval follow-up study is advised to clarify. If initial biopsy findings are negative, a repeat biopsy or close follow-up are required due to the possibility of sampling errors[28] (Fig. 9).

^{68}Ga-DOTA PET/CT in Head and Neck Cancer

Evaluation of head and neck paragangliomas is a common indication for ^{68}Ga-DOTA PET/CT. The neck is the most common primary site for this tumour.[170] Paragangliomas typically present in characteristic locations, with the carotid body being the most common site accounting for over 50% (Fig. 10). They also occur at the jugular foramen, middle ear and along the course of the vagus nerve.[171] They are usually nonfunctioning and benign, demonstrating only local

invasion.[172,173] There are no histopathological criteria to accurately define a malignant paraganglioma and therefore malignancy is defined by the presence of metastases.[174] Less than 5% of paragangliomas of the head and neck metastasize and this number is even lower for carotid body lesions.[170]

^{68}Ga-DOTAPET/CT is the most sensitive tool for the detection of head and neck paragangliomas as they may be very small and difficult to detect.[175]

Approximately 40% of paragangliomas are thought to be hereditary.[176] These familial cases tend to present earlier with a peak of between 30 and 35 years and tend to be multicentric.[177] Succinate dehydrogenase is the most commonly implicated genetic mutation and genetic testing is recommended in all patients depending on local resources.[178]

Conclusion

Incidental findings and technical artifacts are common on ^{18}F-FDG PET/CT and ^{68}Ga-DOTA PET/CT imaging. Comprehensive knowledge of variant physiological biodistribution and potential pitfalls of image interpretation are vital to maximize diagnostic accuracy (Table 2). Patient outcomes can also be improved with appropriate complementary use of structural imaging with either CT, MR or ultrasound in a number of head and neck pathologies.

References

1. Hicks RJ, Hofman MS: Is there still a role for SPECT-CT in oncology in the PET/CT era? Nat Rev Clin Oncol 9:712-720, 2012
2. Hofman MS, Lau WF, Hicks RJ: Somatostatin receptor imaging with 68Ga DOTATATE PET/CT: Clinical utility, normal patterns, pearls, and pitfalls in interpretation. Radiographics 35:500-516, 2015
3. Wahl RL: Targeting glucose transporters for tumor imaging: "Sweet" idea, "sour" result. J Nucl Med 37:1038-1041, 1996
4. Pauwels EK, Ribeiro MJ, Stoot JH, et al: FDG accumulation and tumor biology. Nucl Med Biol 25:317-322, 1998
5. Bar-Shalom R, Valdivia AY, Blaufox MD: PET imaging in oncology. Semin Nucl Med 30:150-185, 2000
6. Czernin J, Phelps ME: Positron emission tomography scanning: Current and future applications. Annu Rev Med 53:89-112, 2002
7. Kapoor V, McCook BM, Torok FS: An introduction to PET/CT imaging. Radiographics 24:523-543, 2004
8. Hicks RJ: Use of molecular targeted agents for the diagnosis, staging and therapy of neuroendocrine malignancy. Cancer Imaging 10:S83-S91, 2010
9. Velikyan I, Sundin A, Sörensen J, et al: Quantitative and qualitative intrapatient comparison of 68Ga-DOTATOC and 68Ga-DOTATATE: net uptake rate for accurate quantification. J Nucl Med 55:204-210, 2014
10. Grégoire V, Leroy R, Heus P, et al: Oropharyngeal, hypopharyngeal and laryngeal cancer: diagnosis, treatment and follow-up. KCE REPORT 256Cs. Belgian Health Care Knowledge Centre, 2015. Available from: https://kce.fgov.be/sites/default/files/atoms/files/KCE_256C_Head-and-neck_cancer_Summary.pdf
11. Fleming AJ Jr, Smith SP Jr, Paul CM, et al: Impact of [18F]-2-Fluorodeoxyglucose–positron emission tomography/computed tomography on previously untreated head and neck cancer patients. Laryngoscope 117:1173-1179, 2007
12. Rohde M, Nielsen AL, Johansen J, et al: Head-to-head comparison of chest X-ray/head and neck MRI, chest CT/head and neck MRI, and (18)F-FDG PET/CT for detection of distant metastases and synchronous cancer in oral, pharyngeal, and laryngeal cancer. J Nucl Med 58:1919-1924, 2017
13. Leroy R, De Gendt C, Stordeur S, et al: Head and neck cancer in Belgium: Quality of diagnostic management and variability across Belgian hospitals between 2009 and 2014. Front Oncol 9:1006, 2019
14. Van den Wyngaert T, De Schepper S, Carp L: Quality assessment in FDG-PET/CT imaging of head-and-neck cancer: one home run is better than two doubles. Front Oncol 10:1458, 2020
15. Mehanna H, McConkey CC, Rahman JK, et al: PET-NECK: a multicentre randomised Phase III non-inferiority trial comparing a positron emission tomography-computerised tomography-guided watch-and-wait policy with planned neck dissection in the management of locally advanced (N2/N3) nodal metastases in patients with squamous cell head and neck cancer. Health Technol Assess 21:1-122, 2017
16. Pfister DG, Spencer S, Adelstein D, et al: Head and neck cancers, Version 2.2020, NCCN Clinical Practice Guidelines in Oncology. J Natl Compr Canc Netw 18:873-898, 2020
17. Virgolini I, Ambrosini V, Bomanji JB, et al: Procedure guidelines for PET/CT tumour imaging with 68Ga-DOTA-conjugated peptides: 68Ga-DOTA-TOC, 68Ga-DOTA-NOC, 68Ga-DOTA-TATE. Eur J Nucl Med Mol Imaging 37:2004-2010, 2010
18. Boellaard R, Delgado-Bolton R, Oyen WJ, et al: FDG PET/CT: EANM procedure guidelines for tumour imaging: version 2.0. Eur J Nucl Med Mol Imaging 42:328-354, 2015
19. Goerres GW, Hany TF, Kamel E, et al: Head and neck imaging with PET and PET/CT: Artefacts from dental metallic implants. Eur J Nucl Med Mol Imaging 29:367-370, 2002
20. Abdoli M, Ay MR, Ahmadian A, et al: Reduction of dental filling metallic artifacts in CT-based attenuation correction of PET data using weighted virtual sinograms optimized by a genetic algorithm. Med Phys 37:6166-6177, 2010
21. Park HH, Shin JY, Lee J, et al: A study on the artifacts generated by dental materials in PET/CT image. In: Annual International Conference of the IEEE Engineering in Medicine and Biology Society IEEE Engineering in Medicine and Biology Society Annual International Conference, 2013:2465-2468, 2013
22. Bujenovic S, Mannting F, Chakrabarti R, et al: Artifactual 2-deoxy-2-[(18)F]fluoro-D-glucose localization surrounding metallic objects in a PET/CT scanner using CT-based attenuation correction. Mol Imaging Biol 5:20-22, 2003
23. Blodgett TM, Ryan A, Akbarpouranbadr A, et al: PET/CT protocols and artifacts in the head and neck. PET Clin 2:433-443, 2007
24. Kamel EM, Burger C, Buck A, et al: Impact of metallic dental implants on CT-based attenuation correction in a combined PET/CT scanner. Eur Radiol 13:724-728, 2003
25. Long NM, Smith CS: Causes and imaging features of false positives and false negatives on 18F-PET/CT in oncologic imaging. Insights Imaging 2:679-698, 2011
26. Nahmias C, Lemmens C, Faul D, et al: Does reducing CT artifacts from dental implants influence the PET interpretation in PET/CT studies of oral cancer and head and neck cancer? J Nucl Med 49:1047-1052, 2008
27. Sureshbabu W, Mawlawi O: PET/CT imaging artifacts. J Nucl Med Technol 33:156-161, 2005
28. Subramaniam RM, Truong M, Peller P, et al: Fluorodeoxyglucose-positron-emission tomography imaging of head and neck squamous cell cancer. Am J Neuroradiol 31:598-604, 2010
29. Blodgett TM, Fukui MB, Snyderman CH, et al: Combined PET/CT in the head and neck: Part 1. Physiologic, altered physiologic, and artifactual FDG uptake. Radiographics 25:897-912, 2005
30. Antoch G, Freudenberg LS, Egelhof T, et al: Focal tracer uptake: a potential artifact in contrast-enhanced dual-modality PET/CT scans. J Nucl Med 43:1339-1342, 2002
31. Kostakoglu L, Wong JC, Barrington SF, et al: Speech-related visualization of laryngeal muscles with fluorine-18-FDG. J Nucl Med 37:1771-1773, 1996
32. Jackson RS, Schlarman TC, Hubble WL, et al: Prevalence and patterns of physiologic muscle uptake detected with whole-body 18F-FDG PET. J Nucl Med Technol 34:29-33, 2006
33. Purohit BS, Ailianou A, Dulguerov N, et al: FDG-PET/CT pitfalls in oncological head and neck imaging. Insights Imaging 5:585-602, 2014

34. Zhu Z, Chou C, Yen TC, et al: Elevated F-18 FDG uptake in laryngeal muscles mimicking thyroid cancer metastases. Clin Nucl Med 26:689-691, 2001
35. Heller MT, Meltzer CC, Fukui MB, et al: Superphysiologic FDG uptake in the non-paralyzed vocal cord. Resolution of a false-positive PET result with combined PET/CT imaging. Clin Positron Imaging 3:207-211, 2000
36. Jacene HA, Goudarzi B, Wahl RL: Scalene muscle uptake: a potential pitfall in head and neck PET/CT. Eur J Nucl Med Mol Imaging 35:89-94, 2008
37. Su H-C, Huang C, Bai Y-L, et al: Physiologically variant FDG uptake in scalene muscle mimicking neck lymph node metastasis in a patient with lung cancer. Ann Nucl Med Sci 22:239-243, 2009
38. Barrington SF, Maisey MN: Skeletal muscle uptake of fluorine-18-FDG: effect of oral diazepam. J Nucl Med 37:1127-1129, 1996
39. Karunanithi S, Soundararajan R, Sharma P, et al: Spectrum of Physiologic and pathologic skeletal muscle (18)F-FDG uptake on PET/CT. Am J Roentgenol 205:W141-W149, 2015
40. Kostakoglu L, Hardoff R, Mirtcheva R, et al: PET/CT fusion imaging in differentiating physiologic from pathologic FDG uptake. Radiographics 24:1411-1431, 2004
41. Bhargava P, Rahman S, Wendt J: Atlas of confounding factors in head and neck PET/CT imaging. Clin Nucl Med 36:e20-e29, 2011
42. Fukui MB, Blodgett TM, Snyderman CH, et al: Combined PET/CT in the head and neck: part 2. Diagnostic uses and pitfalls of oncologic imaging. Radiographics 25:913-930, 2005
43. Kapoor V, Fukui MB, McCook BM: Role of 18F-FDG PET/CT in the treatment of head and neck cancers: Posttherapy evaluation and pitfalls. Am J Roentgenol 184:589-597, 2005
44. Birkin E, Moore KS, Huang C, et al: Determinants of physiological uptake of 18F-fluorodeoxyglucose in palatine tonsils. Medicine (Baltimore) 97:e11040, 2018
45. Pencharz D, Dunn J, Connor S, et al: Palatine tonsil SUVmax on FDG PET/CT as a discriminator between benign and malignant tonsils in patients with and without head and neck squamous cell carcinoma of unknown primary. Clin Radiol 74:165.e17-165.e23, 2019
46. Coelho M, Oliveira T, Fernandes R: Biochemistry of adipose tissue: An endocrine organ. Arch Med Sci 9:191-200, 2013
47. Cronin CG, Prakash P, Daniels GH, et al: Brown fat at PET/CT: Correlation with patient characteristics. Radiology 263:836-842, 2012
48. Paidisetty S, Blodgett TM: Brown fat: Atypical locations and appearances encountered in PET/CT. Am J Roentgenol 193:359-366, 2009
49. Yeung HW, Grewal RK, Gonen M, et al: Patterns of (18)F-FDG uptake in adipose tissue and muscle: A potential source of false-positives for PET. J Nucl Med 44:1789-1796, 2003
50. Cannon B, Nedergaard J: Brown adipose tissue: Function and physiological significance. Physiol Rev 84:277-359, 2004
51. Saito M, Matsushita M, Yoneshiro T, et al: Brown adipose tissue, diet-induced thermogenesis, and thermogenic food ingredients: From mice to men. Front Endocrinol 11:222, 2020
52. Cohade C, Osman M, Pannu HK, et al: Uptake in supraclavicular area fat ("USA-Fat"): Description on 18F-FDG PET/CT. J Nucl Med 44:170-176, 2003
53. Hany TF, Gharehpapagh E, Kamel EM, et al: Brown adipose tissue: A factor to consider in symmetrical tracer uptake in the neck and upper chest region. Eur J Nucl Med Mol Imaging 29:1393-1398, 2002
54. Gelfand MJ, O'Hara S M, Curtwright LA, et al: Pre-medication to block [(18)F]FDG uptake in the brown adipose tissue of pediatric and adolescent patients. Pediatr Radiol 35:984-990, 2005
55. Perkins AC, Mshelia DS, Symonds ME, et al: Prevalence and pattern of brown adipose tissue distribution of 18F-FDG in patients undergoing PET/CT in a subtropical climatic zone. Nucl Med Commun 34:168-174, 2013
56. Hull D, Segall MM: Sympathetic nervous control of brown adipose tissue and heat production in the new-born rabbit. J Physiol 181:458-467, 1965
57. Cousins J, Czachowski M, Muthukrishnan A, et al: Pediatric brown adipose tissue on (18)F-FDG PET: diazepam intervention. J Nucl Med Technol 45:82-86, 2017
58. Söderlund V, Larsson SA, Jacobsson H: Reduction of FDG uptake in brown adipose tissue in clinical patients by a single dose of propranolol. Eur J Nucl Med Mol Imaging 34:1018-1022, 2007
59. Viglianti B, Wong KK, Gross M, et al: Common pitfalls in oncologic FDG PET/CT Imaging. J Am Osteopath Coll Radiol 7:5-17, 2018
60. Adelstein D, Gillison ML, Pfister DG, et al: NCCN Guidelines Insights: Head and Neck Cancers, Version 2.2017. J Natl Compr Canc Netw 15:761-770, 2017
61. Siegel RL, Miller KD, Jemal A: Cancer statistics, 2016. CA Cancer J Clin 66:7-30, 2016
62. Brierley JD, Gospodarowicz MK, Wittekind C (eds): TNM Classification of Malignant Tumours (Eighth edition), Oxford, UK Hoboken NJ: John Wiley & Sons, Ltd, 2017
63. Amin MB, Greene FL, Edge SB, et al: The eighth edition AJCC cancer staging manual: Continuing to build a bridge from a population-based to a more "personalized" approach to cancer staging. CA Cancer J Clin 67:93-99, 2017
64. Goerres GW, Schuknecht B, Schmid DT, et al: Positron emission tomography/computed tomography for staging and restaging of head and neck cancer: Comparison with positron emission tomography read together with contrast-enhanced computed tomography. Clin Imaging 32:431-437, 2008
65. Pentenero M, Cistaro A, Brusa M, et al: Accuracy of 18F-FDG-PET/CT for staging of oral squamous cell carcinoma. Head Neck 30:1488-1496, 2008
66. Veit-Haibach P, Luczak C, Wanke I, et al: TNM staging with FDG-PET/CT in patients with primary head and neck cancer. Eur J Nucl Med Mol Imaging 34:1953-1962, 2007
67. Ong CK, Chong VF: Imaging of tongue carcinoma. Cancer Imaging 6:186-193, 2006
68. Goerres GW, Schmid DT, Schuknecht B, et al: Bone invasion in patients with oral cavity cancer: Comparison of conventional CT with PET/CT and SPECT/CT. Radiology 237:281-287, 2005
69. Gu DH, Yoon DY, Park CH, et al: CT, MR, (18)F-FDG PET/CT, and their combined use for the assessment of mandibular invasion by squamous cell carcinomas of the oral cavity. Acta Radiol 51:1111-1119, 2010
70. Tantiwongkosi B, Yu F, Kanard A, et al: Role of (18)F-FDG PET/CT in pre and post treatment evaluation in head and neck carcinoma. World J Radiol 6:177-191, 2014
71. Paes FM, Singer AD, Checkver AN, et al: Perineural spread in head and neck malignancies: Clinical significance and evaluation with 18F-FDG PET/CT. Radiographics 33:1717-1736, 2013
72. Collazo-Clavell ML, Gharib H, Maragos NE: Relationship between vocal cord paralysis and benign thyroid disease. Head Neck 17:24-30, 1995
73. Myssiorek D: Recurrent laryngeal nerve paralysis: Anatomy and etiology. Otolaryngol Clin North Am 37:25-44, 2004
74. Rosenthal LH, Benninger MS, Deeb RH: Vocal fold immobility: A longitudinal analysis of etiology over 20 years. Laryngoscope 117:1864-1870, 2007
75. Dankbaar JW, Pameijer FA: Vocal cord paralysis: Anatomy, imaging and pathology. Insights Imaging 5:743-751, 2014
76. Chin SC, Edelstein S, Chen CY, et al: Using CT to localize side and level of vocal cord paralysis. AJR Am J Roentgenol 180:1165-1170, 2003
77. Paquette CM, Manos DC, Psooy BJ: Unilateral vocal cord paralysis: A review of CT findings, mediastinal causes, and the course of the recurrent laryngeal nerves. Radiographics 32:721-740, 2012
78. Agha FP: Recurrent laryngeal nerve paralysis: A laryngographic and computed tomographic study. Radiology 148:149-155, 1983
79. Bae JS, Chae BJ, Park WC, et al: Incidental thyroid lesions detected by FDG-PET/CT: Prevalence and risk of thyroid cancer. World J Surg Oncol 7:63, 2009
80. Kim TY, Kim WB, Ryu JS, et al: 18F-fluorodeoxyglucose uptake in thyroid from positron emission tomogram (PET) for evaluation in cancer patients: High prevalence of malignancy in thyroid PET incidentaloma. Laryngoscope 115:1074-1078, 2005
81. Liu Y: Clinical significance of thyroid uptake on F18-fluorodeoxyglucose positron emission tomography. Ann Nucl Med 23:17-23, 2009

82. Nakamoto Y, Tatsumi M, Hammoud D, et al: Normal FDG distribution patterns in the head and neck: PET/CT evaluation. Radiology 234:879-885, 2005
83. Are C, Hsu JF, Schoder H, et al: FDG-PET detected thyroid incidentalomas: Need for further investigation? Ann Surg Oncol 14:239-247, 2007
84. Chen YK, Ding HJ, Chen KT, et al: Prevalence and risk of cancer of focal thyroid incidentaloma identified by 18F-fluorodeoxyglucose positron emission tomography for cancer screening in healthy subjects. Anticancer Res 25:1421-1426, 2005
85. Chu QD, Connor MS, Lilien DL, et al: Positron emission tomography (PET) positive thyroid incidentaloma: The risk of malignancy observed in a tertiary referral center. Am Surg 72:272-275, 2006
86. Cohen MS, Arslan N, Dehdashti F, et al: Risk of malignancy in thyroid incidentalomas identified by fluorodeoxyglucose-positron emission tomography. Surgery 130:941-946, 2001
87. Kang KW, Kim SK, Kang HS, et al: Prevalence and risk of cancer of focal thyroid incidentaloma identified by 18F-fluorodeoxyglucose positron emission tomography for metastasis evaluation and cancer screening in healthy subjects. J Clin Endocrinol Metab 88:4100-4104, 2003
88. Yi JG, Marom EM, Munden RF, et al: Focal uptake of fluorodeoxyglucose by the thyroid in patients undergoing initial disease staging with combined PET/CT for non-small cell lung cancer. Radiology 236:271-275, 2005
89. Erdi YE, Nehmeh SA, Mulnix T, et al: PET performance measurements for an LSO-based combined PET/CT scanner using the National Electrical Manufacturers Association NU 2-2001 standard. J Nucl Med 45:813-821, 2004
90. Chen YK, Chen YL, Cheng RH, et al: The significance of FDG uptake in bilateral thyroid glands. Nucl Med Commun 28:117-122, 2007
91. Gandy N, Arshad MA, Wallitt KL, et al: Immunotherapy-related adverse effects on (18)F-FDG PET/CT imaging. Br J Radiol 93:20190832, 2020
92. Iravani A, Hicks RJ: Pitfalls and immune-related adverse events. In: Lopci E, Fanti S (eds): Atlas of Response to Immunotherapy, Cham Switzerland: Springer Nature Switzerland AG, 2020
93. Karantanis D, Bogsrud TV, Wiseman GA, et al: Clinical significance of diffusely increased ^{18}F-FDG uptake in the thyroid gland. J Nucl Med 48:896-901, 2007
94. Kurata S, Ishibashi M, Hiromatsu Y, et al: Diffuse and diffuse-plus-focal uptake in the thyroid gland identified by using FDG-PET: Prevalence of thyroid cancer and Hashimoto's thyroiditis. Ann Nucl Med 21:325-330, 2007
95. Wachsmann JW, Ganti R, Peng F: Immune-mediated disease in ipilimumab immunotherapy of melanoma with FDG PET/CT. Acad Radiol 24:111-115, 2017
96. Yasuda S, Shohtsu A, Ide M, et al: Chronic thyroiditis: diffuse uptake of FDG at PET. Radiology 207:775-778, 1998
97. Chen YK, Wang YF, Chiu JS: Diagnostic trinity: Graves' disease on F-18 FDG PET. Clin Nucl Med 32:816-817, 2007
98. Shreve PD, Anzai Y, Wahl RL: Pitfalls in oncologic diagnosis with FDG PET imaging: physiologic and benign variants. Radiographics 19:61-77, 1999. quiz 150-1
99. Börner AR, Voth E, Wienhard K, et al: F-18-FDG PET in autonomous goiter. Nuklearmedizin 38:1-6, 1999
100. Bogsrud TV, Karantanis D, Nathan MA, et al: The value of quantifying 18F-FDG uptake in thyroid nodules found incidentally on whole-body PET/CT. Nucl Med Commun 28:373-381, 2007
101. Choi JY, Lee KS, Kim HJ, et al: Focal thyroid lesions incidentally identified by integrated 18F-FDG PET/CT: Clinical significance and improved characterization. J Nucl Med 47:609-615, 2006
102. Chun AR, Jo HM, Lee SH, et al: Risk of malignancy in thyroid incidentalomas identified by fluorodeoxyglucose-positron emission tomography. Endocrinol Metab 30:71-77, 2015
103. Davis PW, Perrier ND, Adler L, et al: Incidental thyroid carcinoma identified by positron emission tomography scanning obtained for metastatic evaluation. Am Surg 67:582-584, 2001
104. de Geus-Oei LF, Pieters GF, Bonenkamp JJ, et al: 18F-FDG PET reduces unnecessary hemithyroidectomies for thyroid nodules with inconclusive cytologic results. J Nucl Med 47:770-775, 2006
105. Ishimori T, Patel PV, Wahl RL: Detection of unexpected additional primary malignancies with PET/CT. J Nucl Med 46:752-757, 2005
106. Kwak JY, Kim EK, Yun M, et al: Thyroid incidentalomas identified by 18F-FDG PET: Sonographic correlation. Am J Roentgenol 191:598-603, 2008
107. Nam SY, Roh J-L, Kim JS, et al: Focal uptake of 18F-fluorodeoxyglucose by thyroid in patients with nonthyroidal head and neck cancers. Clin Endocrinol (Oxf) 67:135-139, 2007
108. Ramos CD, Chisin R, Yeung HW, et al: Incidental focal thyroid uptake on FDG positron emission tomographic scans may represent a second primary tumor. Clin Nucl Med 26:193-197, 2001
109. Sebastianes FM, Cerci JJ, Zanoni PH, et al: Role of 18F-fluorodeoxyglucose positron emission tomography in preoperative assessment of cytologically indeterminate thyroid nodules. J Clin Endocrinol Metab 92:4485-4488, 2007
110. Van den Bruel A, Maes A, De Potter T, et al: Clinical relevance of thyroid fluorodeoxyglucose-whole body positron emission tomography incidentaloma. J Clin Endocrinol Metab 87:1517-1520, 2002
111. Tessler FN, Middleton WD, Grant EG, et al: ACR Thyroid Imaging, Reporting and Data System (TI-RADS): White paper of the ACR TI-RADS Committee. J Am Coll Radiol JACR 14:587-595, 2017
112. Itani M, Felder G, Naeem M, et al: Risk stratification of (18)F-fluorodeoxyglucose-avid thyroid nodules based on ACR thyroid imaging reporting and data system. J Am Coll Radiol 18:388-394, 2020
113. Kelil T, Keraliya AR, Howard SA, et al: Current concepts in the molecular genetics and management of thyroid cancer: An update for radiologists. Radiographics 36:1478-1493, 2016
114. Mazzaferri EL, Kloos RT: Is diagnostic iodine-131 scanning with recombinant human TSH useful in the follow-up of differentiated thyroid cancer after thyroid ablation? J Clin Endocrinol Metab 87:1490-1498, 2002
115. Abraham T, Schöder H: Thyroid cancer—indications and opportunities for positron emission tomography/computed tomography imaging. Semin Nucl Med 41:121-138, 2011
116. Feine U, Lietzenmayer R, Hanke JP, et al: 18FDG whole-body PET in differentiated thyroid carcinoma. Flipflop in uptake patterns of 18FDG and 131-I. Nuklearmedizin 34:127-134, 1995
117. Dong MJ, Liu ZF, Zhao K, et al: Value of 18F-FDG-PET/PET/CT in differentiated thyroid carcinoma with radioiodine-negative whole-body scan: a meta-analysis. Nucl Med Commun 30:639-650, 2009
118. Treglia G, Villani MF, Giordano A, et al: Detection rate of recurrent medullary thyroid carcinoma using fluorine-18 fluorodeoxyglucose positron emission tomography: A meta-analysis. Endocrine 42:535-545, 2012
119. Skoura E, Datseris IE, Rondogianni P, et al: Correlation between calcitonin levels and [(18)F]FDG-PET/CT in the detection of recurrence in patients with sporadic and hereditary medullary thyroid cancer. ISRN Endocrinol 2012:375231, 2012
120. Ong SC, Schöder H, Patel SG, et al: Diagnostic accuracy of 18F-FDG PET in restaging patients with medullary thyroid carcinoma and elevated calcitonin levels. J Nucl Med 48:501-507, 2007
121. Skoura E, Rondogianni P, Alevizaki M, et al: Role of [(18)F]FDG-PET/CT in the detection of occult recurrent medullary thyroid cancer. Nucl Med Commun 31:567-575, 2010
122. Stahl A, Dzewas B, Schwaiger M, et al: Excretion of FDG into saliva and its significance for PET imaging. Nuklearmedizin 41:214-216, 2002
123. Horiuchi M, Yasuda S, Shohtsu A, et al: Four cases of Warthin's tumor of the parotid gland detected with FDG PET. Ann Nucl Med 12:47-50, 1998
124. Matsuda M, Sakamoto H, Okamura T, et al: Positron emission tomographic imaging of pleomorphic adenoma in the parotid gland. Acta Otolaryngol Suppl 538:214-220, 1998
125. Sagowski C, Ussmüller J: Clinical diagnosis of salivary gland sarcoidosis (Heerfordt syndrome). HNO 48:613-615, 2000

126. Castaigne C, Muylle K, Flamen P: Positron emission tomography in head and neck cancer. In: Hermans R (ed): Head and Neck Cancer Imaging, Medical Radiology. Diagnostic Imaging. Berlin, Heidelberg: Springer-Verlag, 2006
127. Schöder H: Head and neck cancer. In: Strauss HW, Mariani G, Volterrani D, Larson SM (eds). Nuclear Oncology: Pathophysiology and Clinical Applications. New York: Springer Science+Business Media, 2013
128. Spiro RH: Salivary neoplasms: Overview of a 35-year experience with 2,807 patients. Head Neck Surg 8:177-184, 1986
129. Wei-Jen S, Nasrin G, Zhuang H, et al: F-18 FDG positron emission tomography demonstrates resolution of non-Hodgkin's lymphoma of the parotid gland in a patient with Sjogren's syndrome: before and after anti-CD20 antibody rituximab therapy. Clin Nucl Med 27:142-143, 2002
130. Keyes JW, Jr., Harkness BA, Greven K, et al: Salivary gland tumors: pretherapy evaluation with PET. Radiology 192:99-102, 1994
131. Okamura T, Kawabe J, Koyama K, et al: Fluorine-18 fluorodeoxyglucose positron emission tomography imaging of parotid mass lesions. Acta Otolaryngol Suppl 538:209-213, 1998
132. Roh JL, Ryu CH, Choi SH, et al: Clinical utility of 18F-FDG PET for patients with salivary gland malignancies. J Nucl Med 48:240-246, 2007
133. Basu S, Houseni M, Alavi A: Significance of incidental fluorodeoxyglucose uptake in the parotid glands and its impact on patient management. Nucl Med Commun 29:367-373, 2008
134. Kendi ATK, Magliocca KR, Corey A, et al: Is There a Role for PET/CT parameters to characterize benign, malignant, and metastatic parotid tumors? Am J Roentgenol 207:635-640, 2016
135. Gillison ML, D'Souza G, Westra W, et al: Distinct risk factor profiles for human papillomavirus type 16-positive and human papillomavirus type 16-negative head and neck cancers. J Natl Cancer Inst 100:407-420, 2008
136. Benard VB, Johnson CJ, Thompson TD, et al: Examining the association between socioeconomic status and potential human papillomavirus-associated cancers. Cancer 113:2910-2918, 2008
137. Chaturvedi AK, Engels EA, Anderson WF, et al: Incidence trends for human papillomavirus-related and -unrelated oral squamous cell carcinomas in the United States. J Clin Oncol 26:612-619, 2008
138. D'Souza G, Kreimer AR, Viscidi R, et al: Case-control study of human papillomavirus and oropharyngeal cancer. N Engl J Med 356:1944-1956, 2007
139. Ang KK, Harris J, Wheeler R, Weber R, et al: Human papillomavirus and survival of patients with oropharyngeal cancer. N Engl J Med 363:24-35, 2010
140. Van Dyne EA, Henley SJ, Saraiya M, et al: Trends in human papillomavirus-associated cancers - United States, 1999-2015. Morb Mortal Wkly Rep 67:918-924, 2018
141. Settle K, Posner MR, Schumaker LM, et al: Racial survival disparity in head and neck cancer results from low prevalence of human papillomavirus infection in black oropharyngeal cancer patients. Cancer Prev Res (Phila) 2:776-781, 2009
142. O'Sullivan B, Huang SH, Su J, et al: Development and validation of a staging system for HPV-related oropharyngeal cancer by the International Collaboration on Oropharyngeal cancer Network for Staging (ICON-S): A multicentre cohort study. Lancet Oncol 17:440-451, 2016
143. Haughey BH, Sinha P, Kallogjeri D, et al: Pathology-based staging for HPV-positive squamous carcinoma of the oropharynx. Oral Oncol 62:11-19, 2016
144. Glastonbury CM: Head and neck squamous cell cancer: Approach to staging and surveillance. In: Hodler J, Kubik-Huch RA, von Schulthess GK (eds): Diseases of the Brain, Head and Neck, Spine 2020—2023: Diagnostic Imaging. Cham Switzerland: Springer Nature Switzerland AG, 2020
145. Hannah A, Scott AM, Tochon-Danguy H, et al: Evaluation of 18 F-fluorodeoxyglucose positron emission tomography and computed tomography with histopathologic correlation in the initial staging of head and neck cancer. Ann Surg 236:208-217, 2002
146. Nabili V, Zaia B, Blackwell KE, et al: Positron emission tomography: Poor sensitivity for occult tonsillar cancer. Am J Otolaryngol 28:153-157, 2007
147. Gray BR, Koontz NA: Normal patterns and pitfalls of FDG uptake in the head and neck. Semin Ultrasound CT MR 40:367-375, 2019
148. Goldenberg D, Begum S, Westra WH, et al: Cystic lymph node metastasis in patients with head and neck cancer: An HPV-associated phenomenon. Head Neck 30:898-903, 2008
149. Morani AC, Eisbruch A, Carey TE, et al: Intranodal cystic changes: a potential radiologic signature/biomarker to assess the human papillomavirus status of cases with oropharyngeal malignancies. J Comput Assist Tomogr 37:343-345, 2013
150. Sakai O, Curtin HD, Romo LV, et al: Lymph node pathology. Benign proliferative, lymphoma, and metastatic disease. Radiol Clin North Am 38:979-998, 2000
151. van den Brekel MW, Stel HV, Castelijns JA, et al: Cervical lymph node metastasis: assessment of radiologic criteria. Radiology 177:379-384, 1990
152. Gordin A, Golz A, Keidar Z, et al: The role of FDG-PET/CT imaging in head and neck malignant conditions: Impact on diagnostic accuracy and patient care. Otolaryngol Head Neck Surg 137:130-137, 2007
153. Schwartz DL, Ford E, Rajendran J, et al: FDG-PET/CT imaging for preradiotherapy staging of head-and-neck squamous cell carcinoma. Int J Radiat Oncol Biol Phys 61:129-136, 2005
154. Roh JL, Yeo NK, Kim JS, et al: Utility of 2-[18F] fluoro-2-deoxy-D-glucose positron emission tomography and positron emission tomography/computed tomography imaging in the preoperative staging of head and neck squamous cell carcinoma. Oral Oncol 43:887-893, 2007
155. Braams JW, Pruim J, Freling NJ, et al: Detection of lymph node metastases of squamous-cell cancer of the head and neck with FDG-PET and MRI. J Nucl Med 36:211-216, 1995
156. Castaldi P, Leccisotti L, Bussu F, et al: Role of (18)F-FDG PET/CT in head and neck squamous cell carcinoma. Acta Otorhinolaryngol Ital 33:1-8, 2013
157. Richards PS, Peacock TE: The role of ultrasound in the detection of cervical lymph node metastases in clinically N0 squamous cell carcinoma of the head and neck. Cancer Imaging 7:167-178, 2007
158. de Bree R, Deurloo EE, Snow GB, et al: Screening for distant metastases in patients with head and neck cancer. Laryngoscope 110:397-401, 2000
159. Duprez F, Berwouts D, De Neve W, et al: Distant metastases in head and neck cancer. Head Neck 39:1733-1743, 2017
160. Scott AM, Gunawardana DH, Bartholomeusz D, et al: PET changes management and improves prognostic stratification in patients with head and neck cancer: Results of a multicenter prospective study. J Nucl Med 49:1593-1600, 2008
161. Haerle SK, Schmid DT, Ahmad N, et al: The value of (18)F-FDG PET/CT for the detection of distant metastases in high-risk patients with head and neck squamous cell carcinoma. Oral Oncol 47:653-659, 2011
162. Zhong J, Sundersingh M, Dyker K, et al: Post-treatment FDG PET/CT in head and neck carcinoma: Comparative analysis of 4 qualitative interpretative criteria in a large patient cohort. Sci Rep 10:4086, 2020
163. Sjövall J, Bitzén U, Kjellén E, et al: Qualitative interpretation of PET scans using a Likert scale to assess neck node response to radiotherapy in head and neck cancer. Eur J Nucl Med Mol Imaging 43:609-616, 2016
164. Goel R, Moore W, Sumer B, et al: Clinical practice in PET/CT for the management of head and neck squamous cell cancer. Am J Roentgenol 209:289-303, 2017
165. Lowe VJ, Hebert ME, Anscher MS, et al: Serial evaluation of increased chest wall F-18 Fluorodeoxyglucose (FDG) uptake following radiation therapy in patients with bronchogenic carcinoma. Clin Positron Imaging 1:185-191, 1998

166. Quon A, Fischbein NJ, McDougall IR, et al: Clinical role of 18F-FDG PET/CT in the management of squamous cell carcinoma of the head and neck and thyroid carcinoma. J Nucl Med 48:58S-68S, 2007
167. Andrade RS, Heron DE, Degirmenci B, et al: Posttreatment assessment of response using FDG-PET/CT for patients treated with definitive radiation therapy for head and neck cancers. Int J Radiat Oncol Biol Phys 65:1315-1322, 2006
168. Trosman SJ, Koyfman SA, Ward MC, et al: Effect of human papillomavirus on patterns of distant metastatic failure in oropharyngeal squamous cell carcinoma treated with chemoradiotherapy. JAMA Otolaryngol Head Neck Surg 141:457-462, 2015
169. Lowe VJ, Boyd JH, Dunphy FR, et al: Surveillance for recurrent head and neck cancer using positron emission tomography. J Clin Oncol 18:651-658, 2000
170. Sajid MS, Hamilton G, Baker DM: A multicenter review of carotid body tumour management. Eur J Vasc Endovasc Surg 34:127-130, 2007
171. Thelen J, Bhatt AA: Multimodality imaging of paragangliomas of the head and neck. Insights Imaging 10:29, 2019
172. Lee JH, Barich F, Karnell LH, et al: National Cancer Data Base report on malignant paragangliomas of the head and neck. Cancer 94:730-737, 2002
173. Lam KY, Chan ACL: Paragangliomas: A comparative clinical, histologic, and immunohistochemical study. Int J Surg Pathol 1:111-116, 1993
174. Fliedner SM, Lehnert H, Pacak K: Metastatic paraganglioma. Semin Oncol 37:627-637, 2010
175. Archier A, Varoquaux A, Garrigue P, et al: Prospective comparison of 68Ga-DOTATATE and 18F-FDOPA PET/CT in patients with various pheochromocytomas and paragangliomas with emphasis on sporadic cases. Eur J Nucl Med Mol Imaging 43:1248-1257, 2016
176. Dahia PL: Pheochromocytoma and paraganglioma pathogenesis: Learning from genetic heterogeneity. Nat Rev Cancer 14:108-119, 2014
177. Piccini V, Rapizzi E, Bacca A, et al: Head and neck paragangliomas: Genetic spectrum and clinical variability in 79 consecutive patients. Endocr Relat Cancer 19:149-155, 2012
178. Lam AK: Update on Adrenal Tumours in 2017 World Health Organization (WHO) of Endocrine Tumours. Endocr Pathol 28:213-227, 2017.